Inorganic Chemistry

Article

pubs.acs.org/IC

A Metathesis Model for the Dehydrogenative Coupling of Amines with Alcohols and Esters into Carboxamides by Milstein's [Ru(PNN)(CO)(H)] Catalysts

Faraj Hasanayn* and Hassan Harb

Department of Chemistry, The American University of Beirut, Beirut, Lebanon

Supporting Information

ABSTRACT: Milstein's [Ru(PNN)(CO)(H)] catalyst (**1**-Ru) is known to mediate the dehydrogenative coupling of alcohols into esters. When it is used in alcohol–amine mixtures it catalyzes carboxamide formation selectively over esters and imines. The given chemistry is generally accepted to follow metal–ligand cooperation (MLC) mechanisms involving hemiacetals and hemiaminals as intermediates. Using electronic structure DFT methods we investigate alternative, more direct OR/H and NHR/H metal/acyl metathesis routes to coupling that circumvent the intermediacy of the hemiacetal and the hemiaminal. The newly proposed mechanism involves formation of hemiacetaloxide and hemiaminaloxide ion-pairs by addition of an aldehyde (from metal-catalyzed alcohol dehydrogenation) to an octahedral ruthenium-alkoxide or ruthenium-amide intermediate (from alcohol or amine addition to **1**-Ru), followed by simple rearrangement (slippage) within the intact ion-pairs to transfer a hydride from the hemiacetaloxide or hemiaminaloxide to the metal. We show that the computed potential energy surfaces that are sometimes invoked to support the MLC mechanism correspond to indirect routes to metathesis. Both the ion-pair and the MLC routes predict the dehydrogenative coupling of ethanol and methanol into methyl acetate to be kinetically much more favored than the kinetics of formation of *N*-methylacetamide from ethanol and methylamine. However, the calculations provide evidence for the accessibility of a low energy NHR/OR metathesis path that would amidate the ester into the experimentally observed thermodynamically more favored carboxamide product. In fact, **1**-Ru is known to be a catalyst for ester amidation.

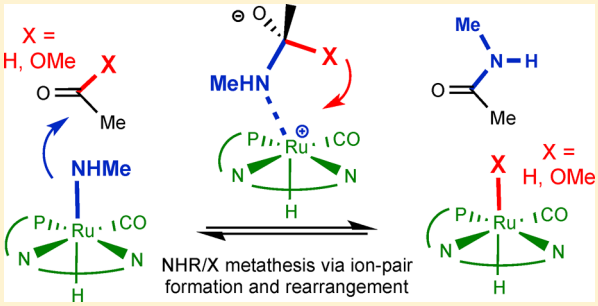

INTRODUCTION

Milstein and co-workers have developed novel methods for making acyl-OR (ester) and acyl-NHR (carboxamide) bonds under neutral conditions by dehydrogenative coupling of alcohols and amines using **1**-Ru and related PNN complexes as catalysts (eqs 1 and 2).[1−3]

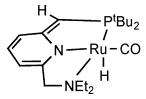

1-Ru

$$2\ RCH_2OH \xrightleftharpoons{\textbf{1}\text{-Ru}} R(C{=}O)OCH_2R + 2\ H_2 \quad (1)$$

$$RCH_2OH + R'NH_2 \xrightleftharpoons{\textbf{1}\text{-Ru}} R(C{=}O)NHR' + 2\ H_2 \quad (2)$$

In an important variation to these reactions, **1**-Ru was shown to catalyze the transesterification[4] and amidation[5] of esters by dehydrogenative coupling with alcohols (eq 3) and amines (eq 4), respectively. These transformations hold great promise as atom economical and environmentally benign methods in organic synthesis as they utilize readily available material and produce H_2 as the only "waste".[6−8]

$$2\ R'OH + R(C{=}O)OCH_2R \xrightleftharpoons{\textbf{1}\text{-Ru}} 2\ R(C{=}O)OR' + 2\ H_2 \quad (3)$$

$$2\ R'NH_2 + R(C{=}O)OCH_2R \xrightleftharpoons{\textbf{1}\text{-Ru}} 2\ R(C{=}O)NHR' + 2\ H_2 \quad (4)$$

The above reactions are done under reflux conditions that expel H_2. Under H_2, **1**-Ru catalyzes the hydrogenation of esters[9] and carboxamides[10] (reverse of eqs 1 and 2). Such hydrogenations are central in organic synthesis[11] but they are typically done stoichiometrically using aluminum or borohydride reagents[12,13] that pose serious environmental concerns. Remarkably, catalysts related to **1**-Ru were shown to hydrogenate organic carbonates and carbamates[14] and urea,[15] which are difficult to perform even with stoichiometric hydride reagents.[16]

The mechanism of catalysis by **1**-Ru is not well understood. **1**-Ru is known to add H_2 via a metal–ligand cooperation (MLC) mode involving the phosphine arm of the PNN ligand to give the octahedral ruthenium *trans*-dihydride complex (**2**–Ru-H; eq 5).[1]

Received: April 1, 2014
Published: July 31, 2014

   dx.doi.org/10.1021/ic500743u | *Inorg. Chem.* 2014, 53, 8334–8349

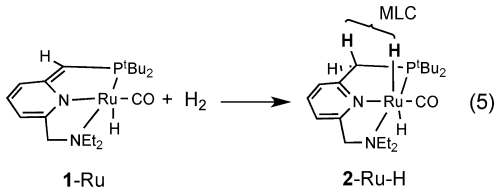

Accordingly, MLC has been systematically assumed to play a role in catalysis.[17,18] For example, hydrogenation of esters and carboxamides is postulated to proceed by an initial MLC reaction utilizing the proton of the phosphine arm of the PNN ligand to give hemiacetals or hemiaminals as intermediates and return **1**-Ru (eqs 6 and 7).[9,10]

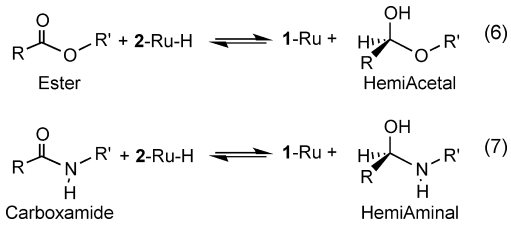

The given MLC reactions are related to the bifunctional reactions invoked by Noyori to account for ketone hydrogenation by octahedral and piano stool ruthenium-amino hydride catalysts (HRu-NH) where the amino group serves as the proton donor (Scheme 1).[19,20] Noyori proposed bifunctional hydrogenation to take place in an outer-sphere mode without prior coordination of the ketone to the metal (Scheme 1).

Scheme 1. Noyori's Bifunctional Mechanism for Ketone Hydrogenation

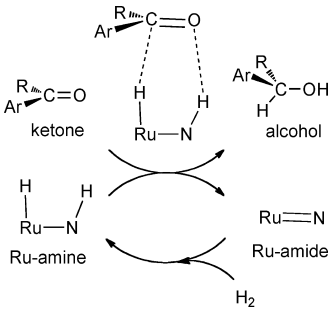

Unlike ketones, however, complete hydrogenation of esters and carboxamides requires hydrogenolysis of a C—OR or a C—NHR bond at some stage of the reaction. For esters, a hydrogenation mechanism starting in hemiacetal formation can proceed, in principle, via fragmentation of the hemiacetal into an alcohol and an aldehyde (eq 8) without the need of a catalyst.[21] In the presence of H_2, the catalyst is expected to hydrogenate the aldehyde to give a second alcohol molecule.

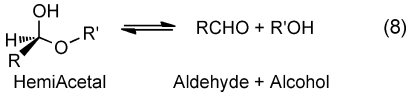

In the absence of a catalyst, hemiaminals, on the other hand, typically undergo dehydration into imines (eq 9).[22]

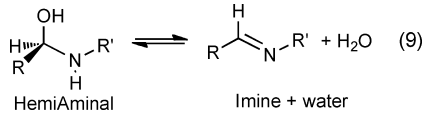

Depending on the catalyst and the reaction conditions, the imine can in turn be hydrogenated into a final amine product.[23,24] No imine or coupled amine products are observed in catalysis by **1**-Ru. In a rather striking effect, however, when the PNP analogue of **1**-Ru is used as the catalyst in amine coupling, imines are observed as the only products.[25] Significantly, although **1**-Ru is a catalyst for alcohol coupling into esters (eq 1), when it is used in the coupling of amines with alcohols, only carboxamides are observed as products.

The possibility of a role for MLC in catalysis by **1**-Ru has been the subject of several theoretical investigations.[26−29] In one study by Wang and co-workers, amine coupling into carboxamides was proposed to proceed according to Scheme 2.[25a]

The scheme begins in two preparatory transformations of the reactants: (i) dehydrogenation of the alcohol into an aldehyde catalyzed by **1**-Ru, and (ii) an MLC addition of the N—H bond of the amine to **1**-Ru to give the octahedral ruthenium-amide (**2**-Ru-NHR). From this point, the carboxamide is formed in two stages. First the aldehyde and the ruthenium-amide are reacted via a six-membered outer-sphere MLC transition state (TS_{HemAm} in Scheme 2 for TS12 in the study by Wang), which was described to make a C—NHR bond concomitantly with proton transfer from the phosphine arm of the PNN ligand to the aldehydic oxygen. Stage 1 produces a hemiaminal and regenerates **1**-Ru. In the second stage **1**-Ru and the hemiaminal are reacted again, but this time via sequential proton and hydride transfer to produce the carboxamide and **2**-Ru-H. A matching scheme was calculated for alcohol coupling into an ester. Based on the computed energy profiles, the study reported that hemiaminal formation and reaction should be kinetically more favored than the reactions involving the hemiacetal, and this was proposed to explain why esters are not observed in the amine-alcohol coupling experiment.

In another theoretical investigation of the same reactions, Li and co-workers considered hemiacetal and hemiaminal formation by condensation of the aldehyde (produced by alcohol dehydrogenation) with an alcohol or an amine without the need of a metal catalyst.[26a] **1**-Ru was then proposed to catalyze hemiaminal and hemiacetal dehydrogenation via sequential MLC proton and hydride transfer steps. This study also reported that carboxamide formation should be kinetically more favored than ester formation. When taken in the directions of ester and carboxamide hydrogenation, the studies of Wang and Li would both start by carbonyl hydrogenation into a hemiacetal or a hemiaminal, but then diverge in how hydrogenolysis takes place.

Under H_2 atmosphere **1**-Ru is transformed quantitatively into **2**-Ru-H (eq 5). NMR and X-ray spectroscopy show the two hydrides in **2**-Ru-H to be in a *trans*-configuration in both solution and the solid phase.[14] The weakening of the two Ru—H bonds in **2**-Ru-H due to their mutual strong trans influence[30,31] is expected to favor hydride transfer to carbonyl compounds via an outer-sphere mode.[32] In a brief communication, we recently reported a detailed analysis of the outer-sphere potential energy surface (PES) of the reaction between the dimethyl amino analogue of **2**-Ru-H and methyl acetate.[33] The results showed that a trivial rearrangement of the hemiacetaloxide formed after hydride transfer from the metal to the carbonyl leads to direct cleavage of the C—OR bond to

dx.doi.org/10.1021/ic500743u | Inorg. Chem. 2014, 53, 8334−8349

Scheme 2. Outline of an MLC Mechanism for Amine-Alcohol Coupling Catalyzed by 1-Ru

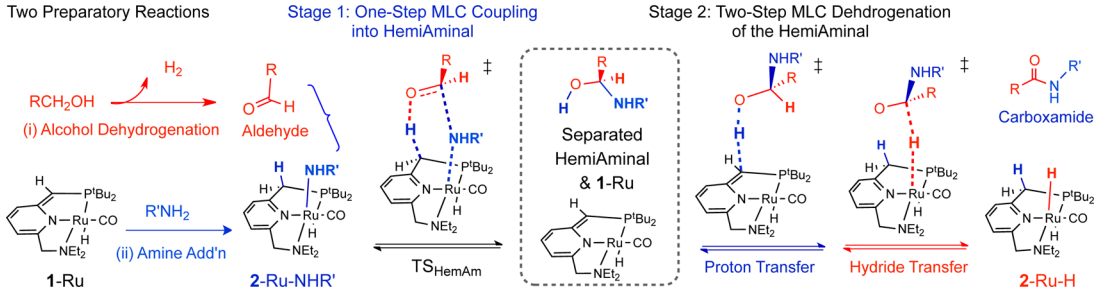

give the octahedral ruthenium-alkoxide (**2**-Ru-OMe; Scheme 3) and eliminate an aldehyde. This transformation is equivalent to

Scheme 3. An Ion-Pair Metathesis Route to Ester Hydrogenation and Transesterification

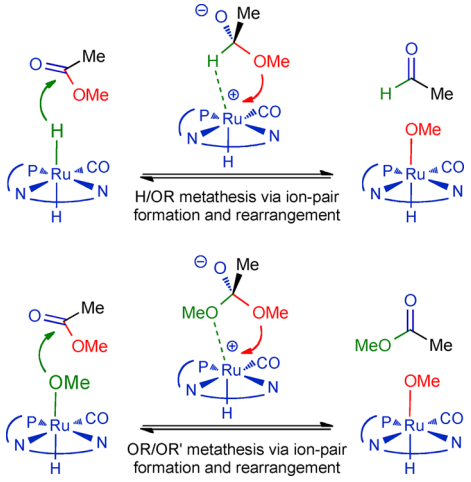

an ion-pair mediated H/OR metathesis in which a hydride and an alkoxide are exchanged between a metal center and an acyl group in an outer-sphere mode. Opposite to MLC, the given mode effectively achieves the hydrogenolysis of the C−OR bond instead of carbonyl hydrogenation.

The calculations also characterized a low energy OR/OR′ metathesis path for exchange of two alkoxides between a metal and an ester (Scheme 3), which we proposed could account for the observed transesterification in eq 3. A separate study identified a low energy H/OR ion-pair metathesis route in the reaction between **2**-Ru-H and dimethyl carbonate.[34] The possibility of other reaction mechanisms that circumvent the intermediacy of hemiacetals had been raised by Gusev and co-workers in a ruthenium SNS-pincer system.[35]

The octahedral ruthenium-alkoxide in Scheme 3 is an experimentally known species that can be formed by addition of an alcohol to **1**-Ru. Likewise, some amines, such as anilines with electron-withdrawing groups, react with the PNP analogue of **1**-Ru to give isolable octahedral ruthenium amides.[36] In the present work we extend the use of the calculations to explore a possible role of ion-pair-mediated NHR/H and NHR/OR metathesis routes in the hydrogenation and coupling chemistry of carboxamides. For the hydrogenation of *N*-methylacetamide by **2**-Ru-H, the computed barrier to H/NHR metathesis is found to be substantial, but still competitive with the MLC barrier producing a hemiaminal. However, careful analysis of the MLC PESs shows that a metal-catalyzed fragmentation of the hemiaminal has to take place on the same metathesis PES, as opposed to a distinct (concerted) MLC mode as suggested by TS_{HemAm} in Scheme 2. When the reaction is followed in the coupling direction, our calculations predict that metal-catalyzed ester formation from amine-alcohol mixtures should be kinetically much more favored than carboxamide formation. The calculations provide evidence that relates the observed selectivity to carboxamides to the accessibility of a low energy ion-pair-mediated NHR/OR metathesis path for ester amidation.

Computational Methods and Solvation Models. The study was done on the dimethyl amino analogue of **1**-Ru, but for convenience we use the same notation for both systems. All calculations were carried out using Gaussian 09.[37] Geometry minimization and normal mode vibrational analysis were done in the gas phase at the M06 level,[38] using the 6-31++G(d,p) basis set on the nonmetal elements,[39] and the Hay−Wadt relativistic effective core potential (ECP) on ruthenium,[40] along with a double-ζ basis set augmented with one *f* polarization and one diffuse *d* function (exponents = 1.24 and 0.015, respectively).[41,42] Selected transition states were also used to conduct intrinsic reaction coordinate analysis (IRC).[43] Final electronic energies were obtained using the gas phase geometries at the M06, M06L,[44] and ωB97X-D[45] levels of theory which are among the more popular methods used in computational organometallic chemistry. For this purpose the larger 6-311++G(2d,2p) basis set was used on the nonmetal elements, and an additional *f* polarization function with exponent = 0.4 was added to Ru. The reported standard state Gibbs free energies were obtained at 298 K and 1 atm using the entropies from the gas phase calculations after scaling them by a factor of 0.5. The reason for scaling the entropies in associative reactions is discussed in the studies by Wang.[25] The scaling factor influences the absolute free energies of the transition states of interest but does not change the main conclusions of the study.

Experimentally, much of the hydrogenation and coupling chemistry of **1**-Ru had been done using toluene as solvent, though some experiments had been also carried out in THF, dioxane, DMSO, and anisole, or without a solvent.[1−3] In the present study two approximation levels are applied to model the solvent. In one, bulk solvent effects are included using the SMD model,[46] with toluene, THF, or methanol as the solvent continuums. Because alcohols are either reactants or products in the reactions of interest, the second approximation level includes a methanol molecule explicitly in the calculations (along with the solvent continuum) to mimic possible specific H-bonding interactions.

dx.doi.org/10.1021/ic500743u | Inorg. Chem. 2014, 53, 8334−8349

RESULTS AND DISCUSSION

Computed Reaction Energies of 1-Ru. The reactions of the square pyramidal **1**-Ru with H_2, methanol, and methylamine (eqs 10−12) are of central importance to the present study. In Table 1 we compare the free energies of the three

Table 1. Computed ΔG° of H_2, Methanol and Methylamine Addition to 1-Ru[a]

	H_2	MeOH	$MeNH_2$
M06 (toluene)	−3.9	−1.4	+10.5
M06L (toluene)	**-6.6**	**-5.0**	**+6.8**
ωB97X-D (toluene)	−7.1	−3.5	+8.4
M06L (THF)	−7.5	−3.0	+8.7
M06L (methanol)	−7.7	−2.4	+10.8

[a]Results from single-point calculations in a polarizable solvent continuum using geometries minimized in the gas phase at the M06 level.

reactions computed using the M06, M06L, and ωB97X-D density functionals and in different solvent continuums. The values given in the equations are for the M06L-toluene results.

$$\textbf{1}\text{-Ru}+H_2 \rightleftharpoons \textbf{2}\text{-Ru-H} \quad \begin{matrix}\Delta H^\circ = -11.4;\ \Delta S^\circ = +16.2\ \text{eu} \\ \Delta G^\circ = -6.6\ \text{kcal/mol}\end{matrix} \qquad (10)$$

$$\textbf{1}\text{-Ru}+\text{MeOH} \rightleftharpoons \textbf{2a}\text{-Ru-OMe} \quad \begin{matrix}\Delta H^\circ = -11.8;\ \Delta S^\circ = -22.6\ \text{eu} \\ \Delta G^\circ = -5.0\ \text{kcal/mol}\end{matrix} \qquad (11)$$

$$\text{1-Ru}+\text{MeNH}_2 \rightleftharpoons \textbf{2a}\text{-Ru-NHMe} \quad \begin{matrix}\Delta H^\circ = 0.0;\ \Delta S^\circ = -22.7\ \text{eu} \\ \Delta G^\circ = +6.8\ \text{kcal/mol}\end{matrix} \qquad (12)$$

The three methods predict H_2 addition to **1**-Ru to be exoergic by 3.9−7.1 kcal/mol (ΔG° at 298.15 and 1.0 atm). The results are qualitatively consistent with the observation that **1**-Ru adds H_2 readily to give an isolable ruthenium trans-dihydride product. Solutions of **1**-Ru in benzene are also known to react with few equivalents of methanol to give an octahedral ruthenium alkoxide, but this product could not be isolated as a solid. The different methods in Table 1 predict methanol addition to **1**-Ru to be approximately 2 kcal/mol less exoergic than H_2 addition. Finally all of the methods in Table 1 agree that the thermodynamics of methylamine addition to **1**-Ru should be about 12 kcal/mol less favored than methanol addition.

The energies in Table 1 exhibit small dependencies on the choice of the solvent continuum in the calculations. For H_2 addition, changing the continuum from toluene to THF or methanol favors the reaction by ∼1 kcal/mol. In contrast, THF and methanol disfavor methanol and methylamine addition by more than 2 kcal/mol.

For the three reactions in Table 1, the M06 energies are significantly less exoergic than either the M06L or the ωB97X-D ones. As mentioned above, the free energies in Table 1 are obtained after scaling the gas phase entropies by a factor of 0.5. This value is arbitrary and probably exaggerated. If the entropies were scaled by 0.7, ΔG° for methanol addition in toluene at the M06 level would be +1.2 kcal/mol, which would be inconsistent with the experiment. With a scaling factor of 0.7, the M06L and ωB97X-D energies remain exoergic by 2.3 and 0.8 kcal/mol, respectively. Studies by Truhlar[47] and more recently by Gusev[48] (using different basis sets than the ones employed here) showed the M06L functional to be systematically accurate in reproducing experimental enthaplies of organometallic reactions having different characters. A recent theoretical investigation of agostic bonding in nickel complexes by Pudasani and Jenesko showed the M06L results to be in good agreement with those from the high level correlation consistent composite approach for transition metals.[49] Similarly, a comprehensive benchmark study by Remya and Suresh of noncovalent interactions between polar molecules found the M06L functional to be the "best performer" in a comprehensive pool of density functionals.[50] The latter systems are directly relevant to the type of potential energy surfaces elucidated in the present study. Accordingly, we chose to base the discussion in the present work on the M06L energies (with the 0.5 entropy scaling factor), and at the end we give a table that compares the relative energy of the key transition states at different levels and in different solvents. We note that we had completed geometry minimization at the M06 level before the given method-validation studies were published. We verified for select reactions that the same final energies are obtained if the geometries were minimized at the M06L or ωB97X-D levels.

Metathesis in the Hydrogenation Direction. Although the ultimate interest of the present study is the dehydrogenative coupling of alcohols and amines, we find it most useful to approach the problem from the hydrogenation direction starting with the octahedral **2**-Ru-H. Because we are largely after supporting the plausibility of a new reaction mode for the C−OR or C−NHR bond-making or -breaking step in a complex multistage reaction system, we chose to work with the simplest ester and carboxamide, namely methyl acetate (**3**) and *N*-methylacetamide (**4**). Due to the asymmetry of the PNN ligand the two hydrides in **2**-Ru-H are not equivalent. As discussed in more detail before,[33,34] this allows definition of several stereoisomeric outer-sphere pathways in the reaction of **2**-Ru-H with a carbonyl compound. We focus on the pathway that aligns the carbonyl of **3** or **4** along the ruthenium−amine bond of **2**-Ru-H (defined as path **a**) as illustrated in eq 13 for the precomplex between **2**-Ru-H and **3**.[51]

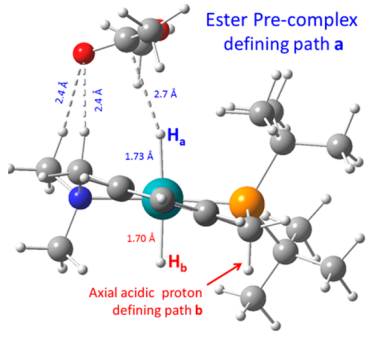

(13)

On this path the carbonyl oxygen is on the opposite side of the axial methylene proton of the phosphine arm that is needed in metal−ligand cooperation, which we denote as path **b** and will be discussed later. The structural and energy data for the stationary points identified on path **a** are given in Figure 1.

The PES in Figure 1 starts with a transition state (**3a**-TS-H) for hydride transfer characterized by a Ru−H and C−H bond distance of 1.94 and 1.42 Å; respectively, and an imaginary frequency of 506i cm^{-1}. **3a**-TS-H leads to an ion-pair minimum between a hemiacetaloxide and a square pyramidal ruthenium cation in which the C−H bond is pointed to the metal at 2.04 Å (**3a**-IP-H). The C−H bond of the hemiacetaloxide anion in **3a**-

dx.doi.org/10.1021/ic500743u | Inorg. Chem. 2014, 53, 8334−8349

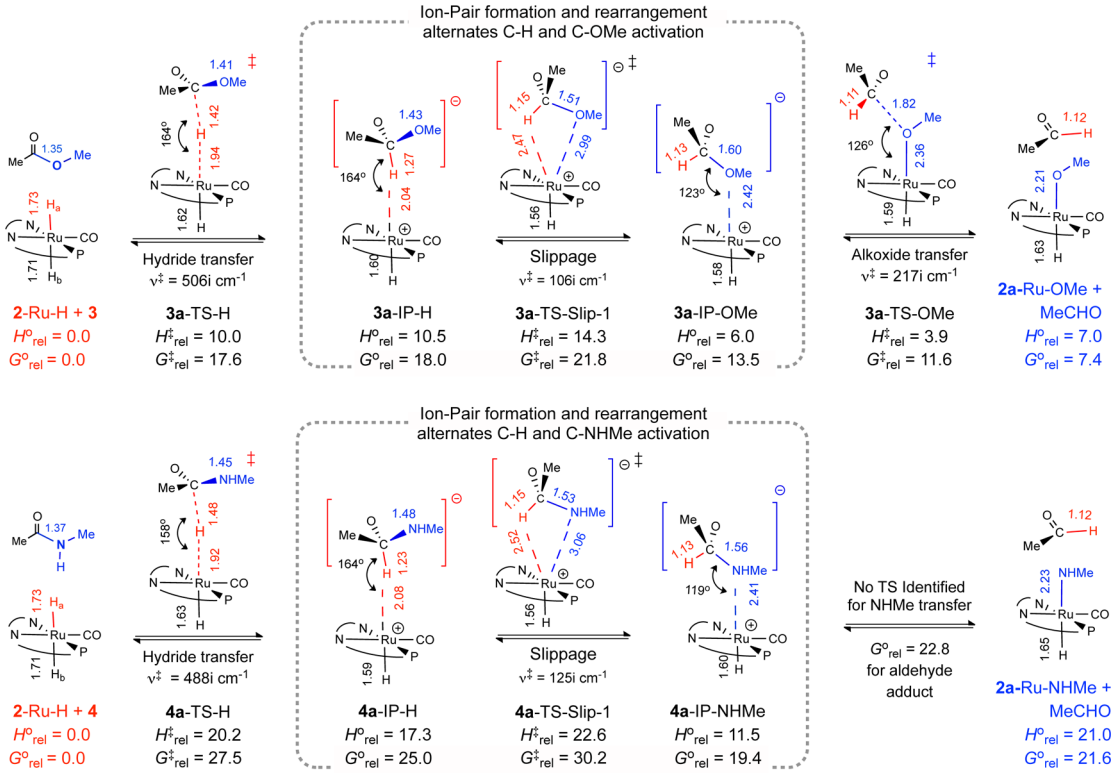

Figure 1. Stationary points on the outer-sphere PES in the reaction of an ester (**3**) and a carboxamide (**4**) with **2**-Ru-H. Energies are given in kcal/mol relative to the separated reactants (M06L-toluene SMD continuum).

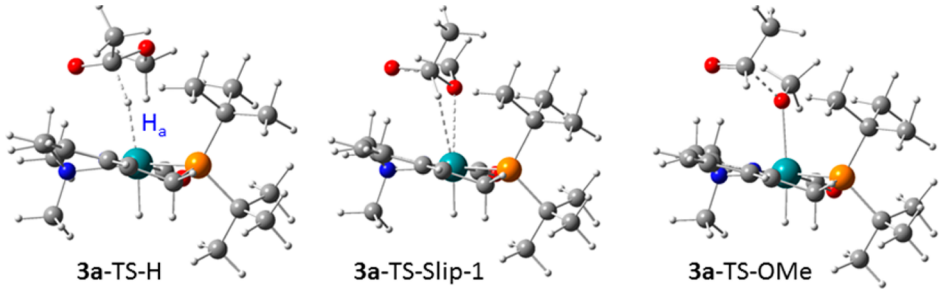

Figure 2. Molecular displays of the three TSs on the metathesis PES of **3**.

IP-H is long (1.27 Å), implicating some degree of activation due to metal coordination. The proposed H/OR metathesis pertains to rearrangement of the ion-pair to coordinate the OMe group of the hemiacetaloxide to the metal in place of the α-hydrogen. The PES has a minimum for the latter species (**3a**-IP-OMe) characterized by a relatively long Ru−OMe bond (2.42 Å), and, more importantly, a significant stretch of the C−OMe bond to 1.60 Å. The computed stretch implies that coordination of the OMe group to the metal activates the C−OMe bond just as it does for the C−H bond in **3a**-IP-H. From **3a**-IP-OMe, the gas phase calculations identify a TS for C−OMe cleavage (**3a**-TS-OMe) that mirrors the hydride transfer TS. **3a**-TS-OMe can be thought to "transfer" an alkoxide from the hemiacetaloxide to the metal to give the octahedral **2a**-Ru-OMe and eliminate acetaldehyde.

The net reaction of **3** in Figure 1 is a metathesis exchanging a hydride and an alkoxide between the metal center of **2**-Ru-H and the acyl group of the ester. The given reaction requires a "mechanism" to alternate the coordination of the C−H and C−OMe groups of the hemiacetaloxide to the metal. In Figure 1 we consider a transition state (**3a**-TS-Slip-1) that achieves the rearrangement in a direct way within the intact ion-pair by pointing both the α-H and the OMe groups of the hemiacetaloxide to the metal. The Ru−H (2.47 Å), C−H (1.13 Å), C−OMe (1.51 Å) and Ru−OMe (2.99 Å) parameters in **3a**-TS-Slip-1 are all intermediate between the corresponding values in the C−H and C−OMe ion-pair. The 3-D molecular displays given in Figure 2 reveal a good structural fit of the hemiacetaloxide in the catalyst "cavity" in each of the three TSs on the metathesis PES.

The computed enthalpy and free energy of the precomplex between the ester and **2**-Ru-H in eq 13 are −3.5 and 3.9 kcal/mol, respectively (M06L, in toluene continuum). The barrier for hydride transfer relative to the separated reactants is 17.6 kcal/mol. This is a relatively low barrier, a result that can be attributed to two factors: (i) an electronic one following from the trans-configuration of the two hydrides in **2**-Ru-H,[33,34,34] and (ii) a structural factor following from the presence of an opening over the amino group which clearly allows the ester to approach the hydride without much steric demand (Figure 2).

dx.doi.org/10.1021/ic500743u | Inorg. Chem. 2014, 53, 8334−8349

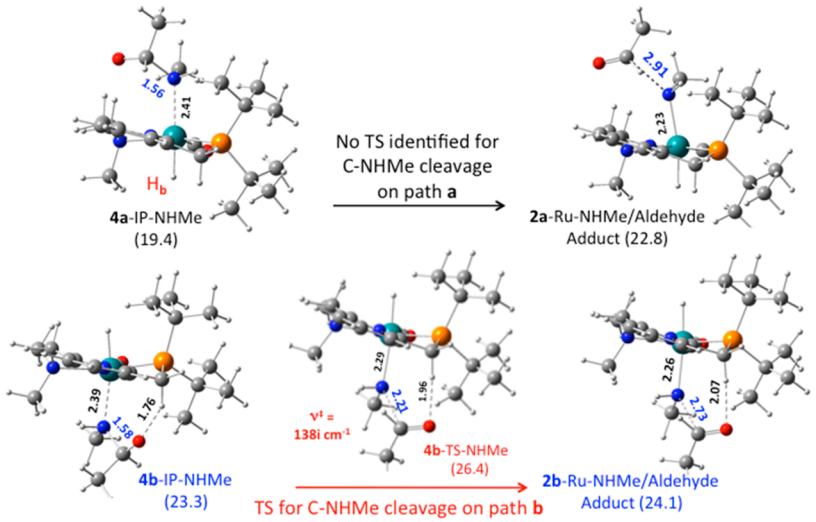

Figure 3. Comparison of C−NHMe bond cleavage of the amine-bound hemiaminaloxide ion-pair on paths **a** and **b**. Energies are given in kcal/mol, and distances in Å.

The C−H bound ion-pair minimum has an energy nearly identical to that of **3a**-TS-H, and from this point the barrier to rearrangement via **3a**-TS-Slip-1 is only 3.8 kcal/mol. The OMe bound ion-pair is 4.5 kcal/mol more stable than **3a**-IP-H, which seems consistent with the better coordinating ability of an OMe group compared to a C−H bond. From **3a**-IP-OMe the gas phase M06 electronic barrier to C−OMe cleavage via **3a**-TS-OMe is just 0.5 kcal/mol. IRC calculations in the gas phase starting from **3a**-TS-OMe confirm the connectivity (Figure S1 in the Supporting Information [SI]) and supports the near absence of a barrier. The barrier for C−OMe dissociation becomes slightly negative when the thermal enthalpic terms and solvent effects are included via single point M06L calculations. In fact, for many of the other stereoisomeric paths the calculations failed to identify a TS for C−OMe cleavage due to the flatness of the PES of the C−OMe cleavage step. We recommend that a relaxed scan of the PES as a function of the C−OR bond distance is used before seeking to identify TSs related to **3a**-TS-OMe. Complete aldehyde elimination from **3a**-IP-OMe is exoergic by 6.1 kcal/mol. The similar energy of each C−H and OMe ion-pair and the corresponding C−H and C−OMe TS indicates that the given ion-pairs themselves can be viewed as activated species on the PES, meaning that once the hydrogen or the OMe group of the α-carbon of the hemiacetaloxide gets into the vicinity of the metal center, it will undergo a barrierless downhill C−H or C−OMe cleavage (corresponding, respectively, to hydride or alkoxide transfer to the metal). Under this condition, **3a**-TS-Slip-1 is the highest energy point on the metathesis PES with $G^{\ddagger}_{rel}$ = 21.8 kcal/mol relative to the separated reactants. This means the direct ion-pair mediated H/OR metathesis of esters can be a chemically relevant reaction even at ambient temperatures.

As found for the ester, the PES in the reaction between *N*-methylacetamide (**4**) and **2**-Ru-H in Figure 1 also starts with a precomplex followed by a hydride transfer TS (**4a**-TS-H) leading to a C−H bound hemiaminaloxide ion-pair minimum (**4a**-IP-H). The barrier for hydride transfer to **4** is much larger than in the reaction of **3**. As found for the ester, the energy of the TS and the C−H ion-pair minimum of **4** are close: 27.5 and 25.0 kcal/mol, respectively.

A "stepwise" ion-pair mediated metathesis starting with the carboxamide requires coordination of the amino nitrogen of the hemiaminaloxide to the metal. A minimum for the latter species (**4a**-IP-NHMe; Figure 1) is computed to have G°_{rel} = 19.4 kcal/mol, a full 5.6 kcal/mol *lower* than the preceding C−H bound ion-pair, which is reasonable, given that the amino group is a classical two-electron donor ligand. In spite of the favorable thermodynamics, however, the barrier for the direct slippage step from **4a**-IP-H to **4a**-IP-NHMe via **4a**-TS-Slip-1 is 5.2 kcal/mol, slightly larger than the matching barrier for hemiacetaloxide slippage (3.8 kcal/mol). The TS structures suggest the difference could follow from slightly greater steric demands in **4a**-TS-Slip-1 due to the additional hydrogen of the NHMe group. With an increased energy input in both the hydride transfer and the slippage components of the H/NHMe metathesis, $G^{\ddagger}_{rel}$ of **4a**-TS-Slip-1 comes to 30.2 kcal/mol. This is a quite substantial barrier, but it is still not prohibitive for the reaction to be chemically relevant under the conditions used in the hydrogenation of carboxamides, which are typically done at temperatures greater than 100 °C and reaction times in the hours.

Upon slippage from **4a**-IP-H to **4a**-IP-NHMe the C−H bond of the hemiaminaloxide contracts from 1.23 to 1.13 Å, whereas the C−NHMe bond lengthens from 1.48 to 1.56 Å. This suggests that coordination of the amino group to the metal weakens the C−NHMe bond, but not to the same extent computed for C−OR activation. However, full C−NHMe bond cleavage starting from **4a**-IP-NHMe into the separated acetaldehyde and the octahedral **2**-Ru-NHMe products is calculated to be highly *endothermic* (ΔH°_{Diss} = 9.5 kcal/mol). Thus, even with the favorable dissociation entropy term (scaled by 0.5) acetaldehyde elimination from **4a**-IP-NHMe is uphill by 2.2 kcal/mol. This behavior is fundamentally different from C−OMe cleavage, where the corresponding ΔH°_{Diss} and ΔG°_{Diss} starting from **3a**-IP-OMe were 1.0 and −6.1 kcal/mol, respectively. The different thermodynamics of the C−OMe and C−NHMe cleavage reactions raises questions on whether the kinetics of the C−NHMe will encounter an increased barrier or not. As shown in Figure 3, C−NHMe cleavage leads at first to an adduct between acetaldehyde and the octahedral **2a**-Ru-NHMe characterized by an N−C bond distance of 2.91 Å. The transformation from ion-pair **2a**-Ru-NHMe to the

dx.doi.org/10.1021/ic500743u | *Inorg. Chem.* 2014, 53, 8334−8349

adduct is uphill by 3.4 kcal/mol. Our extensive attempts to identify a TS for C−NHMe cleavage from **4a**-IP-NHMe to the adduct have not been successful. A relaxed PES scan as a function of the C−NHMe bond distance supports the absence of any significant barrier to dissociation beyond the uphill thermodynamics. Thus, in Figure 1 we use the energy of the aldehyde adduct (G^{o}_{rel} = 22.8 kcal/mol) as a rough estimate for the energy of the missing **4a**-TS-NHMe. On the basis of the given results we can conclude that the slippage TS is the highest energy point on the direct H/NHMe metathesis PES in Figure 1.

Further investigation of the question of the barrier of the metal-mediated C−NHMe cleavage starting from a higher energy ion-pair on path **b** (**4b**-IP-NHMe; G^{o}_{rel} = 23.3 kcal/mol) identified a TS for C−NHMe cleavage characterized by a C−NHMe bond distance of 2.21 Å and an imaginary frequency of 138i cm^{-1} (**4b**-TS-NHMe; Figure 3). As found on path **a**, C−NHMe cleavage on path **b** leads to an aldehyde adduct of **2b**-Ru-NHMe as a true minimum on the PES but with a slightly higher energy than the adduct on path **a** (G^{o}_{rel} = 24.1 vs 22.8 kcal/mol). Overall, the given data indicate that formation and cleavage of the amine-bound hemiaminaloxide ion-pair on path **b** should be much less favored than that on path **a**. Nevertheless, $G^{‡}_{rel}$ of **4b**-TS-NHMe comes to 26.4 kcal/mol relative to the separated reactants, which is still significantly lower than that of **4a**-TS-Slip-1 on path **a** (30.2 kcal/mol; M06L). We note however that at the ωB97X-D level the energies of the slippage (path **a**) and C−N cleavage (path **b**) TSs become equal ($G^{‡}_{rel}$ = 29.6 kcal/mol). Note that on path **b** the carbonyl oxygen gets close to the axial proton on of the phosphine arm (1.76 Å in **4b**-IP-NHMe and 1.96 Å **4b**-TS-NHMe, but there is no indication of any active role of the ligand in assisting C−NHMe cleavage. In addition, the significantly higher energy of **4b**-IP-NHMe compared to that of **4a**-IP-NHMe (3.9 kcal/mol) suggests an absence of a stabilizing bonding CH−carbonyl interaction.

Intrinsic Reaction Coordinates. To further characterize the PESs elucidated above we conducted IRC analyses starting from **3a**-TS-Slip-1 and **4a**-TS-Slip-1. The calculations were carried out in the gas phase at the same (M06) level used in geometry minimization. The M06 electronic energy along the two IRCs relative to the TSs is plotted in Figure 4. The figure includes 3-D molecular displays of the C−H and C−OMe ion-pairs extracted from the actual IRC outputs. The results

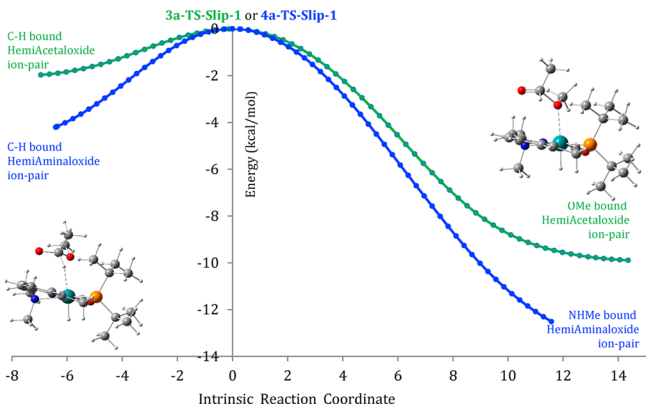

Figure 4. IRCs originating from **3a**-TS-Slip-1 (green curve) and **4a**-TS-Slip-1 (blue curve). M06 gas phase electronic energies are defined relative to the TSs in kcal/mol.

confirm that TS-Slip-1 mediates a direct connection between C−H and C−OMe or C−NHMe "rotamer" ion-pairs. The structural parameters along the two IRCs starting from the C−H ion-pair side reveals smooth contraction of the C−H bond along with a smooth elongation of the C−OMe or C−NHMe bond as TS-Slip-1 is reached and crossed. Finally, the plots reveal a quite flat region of the PES around each of the slippage TSs, which is consistent with the small magnitude of the imaginary frequency in **3a**-TS-Slip-1 and **4a**-**TS**-Slip-1: 106i and 125i cm^{-1}, respectively.

Energy Profiles for full Hydrogenation. Figure 5 compares the Gibbs free energy profiles for complete hydrogenation of **3** and **4**. For convenience, the thermodynamics data for the individual hydrogenation and hydrogenolysis steps are collected in Scheme 4.

Scheme 4. Computed Thermodynamics Data Used in Figure 5 (M06L-Toluene; in kcal/mol)

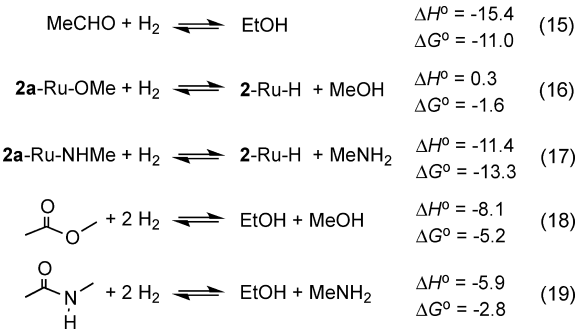

The metathesis in the direction of acetaldehyde formation from **3** and **4** is endoergic by 7.4 and 21.6 kcal/mol, respectively. However, hydrogenation of acetaldehyde is exoergic by 11.0 kcal/mol (eq 15 in Scheme 4), so it provides a major component in driving the hydrogenation thermodynamics of both the ester and the carboxamide.

For complete hydrogenation and catalysis the octahedral **2a**-Ru-OMe and **2a**-Ru-NHMe products must undergo hydrogenolysis to produce an alcohol or an amine and regenerate **2**-Ru-H. These reactions are exoergic by 1.6 and 13.3 kcal/mol, respectively (Table 1 and eqs 16 and 17 in Scheme 4). With these computed energies, the net hydrogenation of methyl acetate and *N*-methylacetamide comes to be exoergic by 5.2 and 2.8 kcal/mol, respectively (eqs 18 and 19 in Scheme 4).

Mechanistically, hydrogenolysis of the Ru−OR and Ru−NHR bonds can proceed in several routes including initial MLC elimination of the alcohol or the amine followed by H_2 addition to the square pyramidal **1**-Ru, direct hydrogenolysis with H_2,[52] and solvent-assisted mechanisms.[53−56] Given the highly favorable thermodynamics and the accessibility of many reaction routes, hydrogenolysis of the Ru−OMe and Ru−NHMe bonds is not expected to be kinetically demanding. Similarly, in the presence of **2**-Ru-H (which should be abundant under high H_2 pressure) hydrogenation of the aldehyde is expected to be fast. For simplicity we keep the barriers for aldehyde hydrogenation out of the PESs in Figure 5. The important point for our purposes is that Figure 5 gives unambiguous evidence that the metathesis route to hydrogenation should be kinetically and thermodynamically much more favored for **3** than for **4**. This may sound trivial since it is well-known that carboxamides are generally much harder to hydrogenate than esters.[16b] However, accepting the large

dx.doi.org/10.1021/ic500743u | Inorg. Chem. 2014, 53, 8334−8349

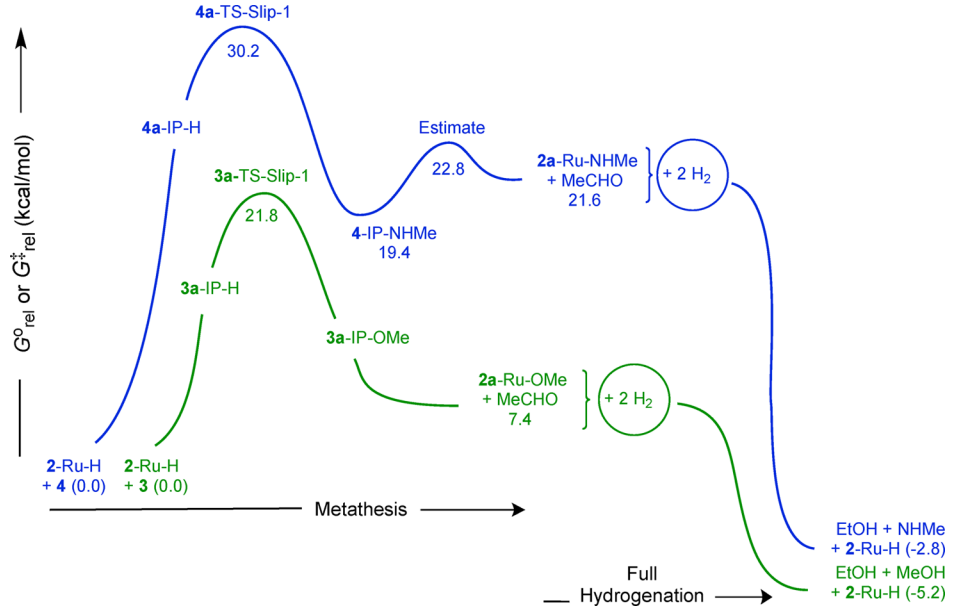

Figure 5. Gibbs free energy profiles (298 K and 1 atm) for the hydrogenation of **3** and **4** using **2**-Ru-H (M06L-toluene; in kcal/mol).

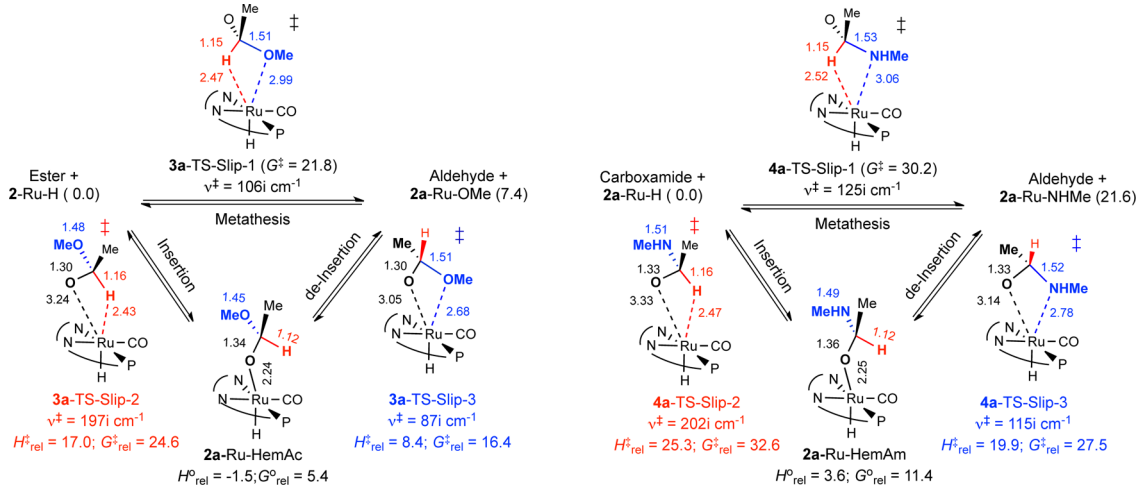

Figure 6. Three ion-pair-mediated reactions. The energies are given in kcal/mol relative to the separated **2**-Ru-H and **3** or **4**.

differences in the hydrogenation PESs becomes critical in the coming discussion of the origin of the observed selectivity to carboxamides over esters in the dehydrogenative coupling of alcohols and amines.

Metathesis via Carbonyl Insertion and Deinsertion. The slippage TSs in Figure 1 alternate the coordination of the C−H bond of a hemiacetaloxide or hemiaminaloxide with an alkoxy or amino group. In Figure 6 we consider another ion-pair rearrangement mode via TS-Slip-2 to coordinate the terminal C−O$^-$ bond of the hemiacetaloxide or hemiaminaloxide to the metal.

The new slippage mode leads to octahedral Ru−hemiacetaloxide and Ru−hemiaminaloxide complexes, **2a**-Ru-HemAc and **2a**-Ru-HemAm, respectively, having Ru−OR bond distances of 2.24 Å, close to the value of 2.21 Å for the Ru−OMe bond in **2a**-Ru-OMe (Figure 1). A molecular display of **2a**-Ru-HemAc is given in eq 20 (without the *tert*-butyl groups).

The reactions mediated by TS-Slip-2 correspond to insertion of a carbonyl group into a Ru−H bond which has ample

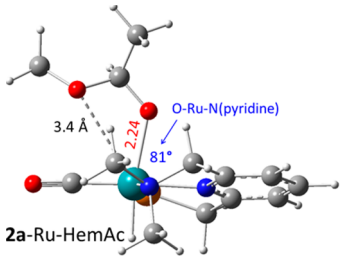

(20)

experimental precedence. Of particular relevance to the present study are the experiments by Bergens, where cyclic esters were observed to undergo rapid insertion in *trans*-[Ru(H)$_2$(Binap)(diamine)] complexes even at low temperatures.[57] The more common examples of carbonyl insertion in octahedral complexes involve ketones[58−60] and CO_2.[61−63] The reverse of the insertion step in Figure 6 is an unconventional β-hydride elimination from an alkoxide taking place via ion-pair rearrangement without the need of a vacant coordination site, which also has experimental precedence.[64−66]

dx.doi.org/10.1021/ic500743u | Inorg. Chem. 2014, 53, 8334−8349

For both **3** and **4** the insertion barrier via TS-Slip-2 is slightly larger than the one for direct metathesis via TS-Slip-1.[67] The thermodynamics of insertion on the other hand are more favored than metathesis, offering G°_{rel} = 5.4 or 11.4 kcal/mol for the reaction of **3** and **4**, respectively. These results imply that insertion can in practice compete with direct metathesis, but it does not provide a thermodynamics sink. However, from the insertion products it is possible to define a third ion-pair rearrangement mode via TS-Slip-3 that exchanges the coordination of the anionic C−O$^-$ terminal of the alkoxide with the alkoxy or the amine group. The 3-D display in eq 20 shows it should not take many structural rearrangements to reach TS-Slip-3. The latter slippage TSs mediate aldehyde deinsertion (or elimination) from **2a**-Ru-HemAc and **2a**-Ru-HemAm. The combined insertion and deinsertion steps provide therefore an indirect ion-pair mediated route to metathesis. $G^{\ddagger}_{rel}$ of **3a**-TS-Slip-3 and **4a**-TS-Slip-3 is 16.4 and 27.5 kcal/mol, respectively, significantly smaller than the other slippage TSs. Thus, even if the kinetics were to favor insertion via TS-Slip-2 over direct metathesis via TS-Slip-1, TS-Slip-3 will still provide an energetically accessible indirect ion-pair-mediated route to metathesis.

IRC calculations starting from **3a**-TS-Slip-2 confirm a smooth connectivity between **3a**-IP-H and **2**-Ru-HemAc. IRC calculations originating in **3a**-TS-Slip-3 on the other hand lead to the insertion product **2a**-Ru-HemAc in one direction, but it converges after two steps to the same geometry as that of **3a**-TS-Slip-3. This behavior may follow from the flat nature of the PES near TS-Slip-3 which is evident from the small magnitude of the imaginary frequency in **3a**-TS-Slip-3 and **4a**-TS-Slip-3, 98i and 115i cm^{-1}, respectively. Animation of these vibrations leaves no doubt they are for a rotation that exchanges the coordination of the terminal O and either the OMe or NHMe group. We have located several stereoisomeric transition states of **3a**-TS-Slip-3 and **4a**-TS-Slip-3, but we could not identify any minima in the close vicinity of any of them. As shown in eq 20, TS-Slip-3 requires minimal structural arrangement of the insertion intermediate, and thus, the IRC result of a minimum near TS-Slip-3 is most likely a computational artifact.

Scheme 5 illustrates stereospecific details pertaining to how the hemiacetaloxide or hemiaminaloxide is produced and transformed on the insertion route to metathesis.

The carbonyl of **3** or **4** approaches **2**-Ru-H from the pyridine side with the alkyl group pointing toward the phosphine group. In TS-Slip-2 the exchanging C−H and C−O$^-$ bonds are aligned along the pyridine−Ru−CO axis, so the C−H bond eclipses the Ru−CO bond. As the Ru−alkoxide bond is formed, the three substituents on the tetrahedral carbon of the alkoxide are rotated so as to stagger the Ru−CO bond in between the C−H and C−X bond (X = OMe or NHMe). Continued rotation eclipses the C−X and Ru−CO bonds, providing thereby the correct alignment needed in TS-Slip-3. In the process, the orientation of the alkyl group is flipped toward the amine, and the aldehyde eliminates from the same side used in the insertion direction. Note that the alkoxide oxygen in **2a**-Ru-HemAc and **2a**-Ru-HemAm is tilted over the pyridyl ring, thus making an O−Ru−N angle of near 80° (eq 20). This structural feature appears to be common in octahedral Ru-alkoxide as was discussed elsewhere.[32]

Effects of an Explicit Solvent Molecule. Complete hydrogenation of **3** and **4** produces methanol. To investigate possible effects of H-bonding of the alcohol on the metathesis PESs, we conducted calculations that included a single methanol molecule to mimic an H-bond solvent donor. Starting with the separated reactants, H-bond formation between methanol and **2**-Ru-H is calculated to be slightly exoergic (ΔG° = −1.4 kcal/mol) so we take this species as the reference point in defining the energies of the other points on the PESs. For each ion-pair the methanol was introduced such that it undergoes an H-bond with the formally "anionic" oxygen center. The results summarized in Figure 7 show the methanol molecule stabilizes all of the ion-pair TSs in the reaction of both **3** and **4** by 3−5 kcal/mol. The effect is not unexpected, since the given reactions replace an H-bond between methanol and a metal-hydride in the reactants by a stronger H-bond involving a negatively charged oxygen in the ion-pair minima and TSs.

Scheme 5. Stereospecific Details of the Insertion−Deinsertion Path to Metathesis

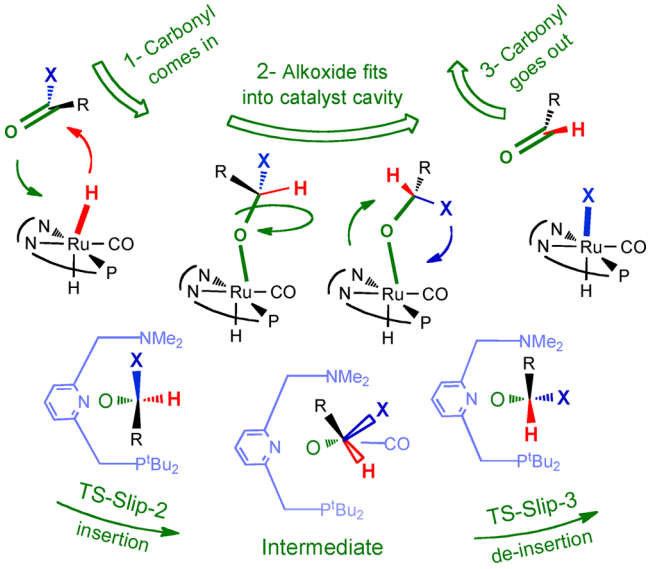

Indirect Metathesis via MLC. In this section we examine more closely the metal−ligand cooperative (MLC) route to hydrogenation. For this purpose Figure 8 tracks an outer-sphere PES that allows interaction between the carbonyl oxygen of **3** or **4** with the axial proton of the phosphine arm of **2**-Ru-H (distinguished as path **b**; see eq 13).

As found in Figure 1, hydride transfer from **2**-Ru-H to methyl acetate on path **b** yields a C−H ion-pair minimum (**3b**-IP-H), but this time the terminal oxygen of the hemiacetaloxide is pointed at the axial C−H proton of the phosphine arm at a distance of 1.94 Å. From **3b**-IP-H, proton transfer from the PNN ligand to the terminal oxygen of the hemiacetaloxide via **3b**-TS-Prt-1 has a barrier of 5.5 kcal/mol. The immediate product from this step is **1b**-Ru-HemAc-1, a loose precomplex between a hemiacetal and the neutral square pyramidal **1**-Ru in which the C−H bond of the hemiacetal is pointed to the metal at a distance of 2.5 Å and the alcoholic proton is at 2.2 Å from the deprotonated carbon of the phosphine arm. $G^{\ddagger}_{rel}$ of **3b**-TS-Prt-1 is 23.8 kcal/mol (in toluene), slightly higher than the energy of **3a**-TS-Slip-1 in Figure 1 (21.8 kcal/mol). Thus, in spite of the very different character of the two reactions, the slippage and ligand deprotonation TSs appear to be competitive. However, for hydrogenation to proceed, the hemiacetal produced after proton transfer would still need to undergo further hydrogenolysis of the C−OR bond. In investigating a possible role of **1**-Ru in the latter reaction we considered the MLC mechanism reported in the study by

dx.doi.org/10.1021/ic500743u | Inorg. Chem. 2014, 53, 8334−8349

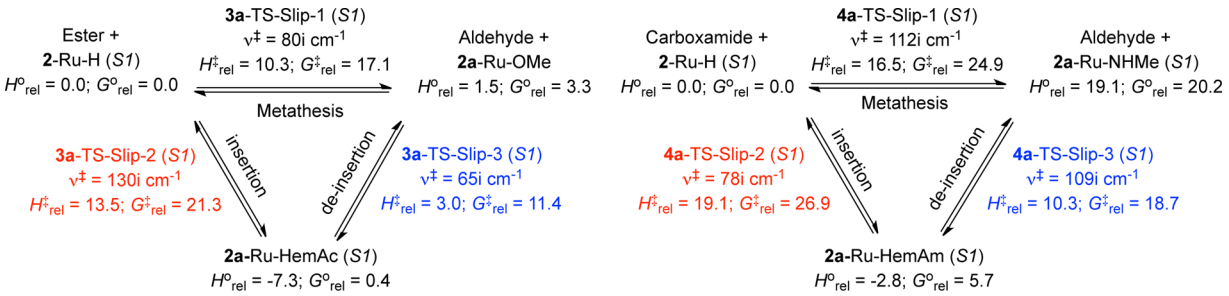

Figure 7. Energies of the slippage TSs computed while including a methanol molecule (*S1*) to mimic an explicit H-bond donor solvent. Free energies are given in kcal/mol relative to the methanol-solvated **2**-Ru-H and either **3** or **4**.

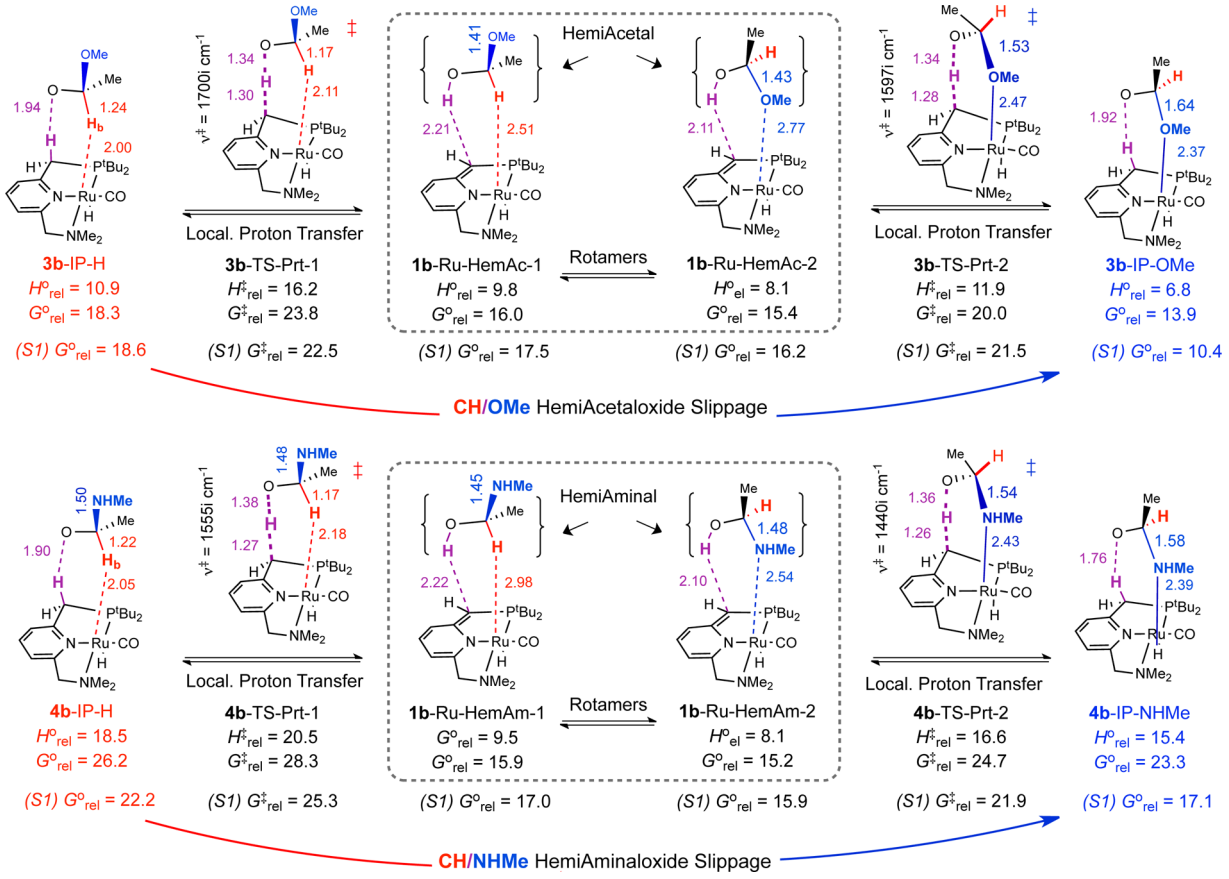

Figure 8. Reaction between **2**-Ru-H and **3** or **4** on path **b** involving ligand deprotonation. The energies are given relative to the separated reactants in kcal/mol. The S1 entries are for reactions including a methanol molecule as an H-donor solvent.

Wang (first stage in Scheme 2 above).[26a] This led us to identify **3b**-TS-Prt-2 in Figure 8 having $G^{\ddagger}_{rel}$ = 20.0 kcal/mol. We find the geometry (near linear C−H−O angle), imaginary frequency (1600i cm^{-1}), reduced mass (1.1 amu), and the animation of the imaginary frequency of **3b**-TS-Prt-2 to be all fully characteristic of a localized motion of the alcoholic proton between an OMe-coordinated hemiacetal precomplex and the carbon of the phosphine arm. This differs from the delocalized description of the same TS in which the C−OR bond is cleaved concomitantly with proton transfer.[26a] Consistent with a localized proton transfer step, Figure 8 shows **3b**-TS-Prt-2 to connect an OMe-coordinated conformer of a hemiacetal precomplex of **1**-Ru (**1b**-Ru-HemAc-2) with an OMe-coordinated hemiacetaloxide ion-pair (**3b**-IP-OMe).[68] This means that the combined MLC sequence of hemiacetal formation and subsequent reaction with **1**-Ru simply switches the C−H coordination of the hemiacetaloxide produced right after hydride transfer into the more favorable mode in which the OMe group points to the metal. In other words the given deprotonation and protonation sequence of the ligand provides an indirect route to interchanging the C−H and C−OMe ion-pairs taking place on path **b**. Further cleavage of the C−OMe bond from **3b**-IP-OMe will complete an MLC-mediated H/OR metathesis. The same is true for the sequence involving the reaction of the carboxamide in Figure 8, where a hemiaminal is formed by ligand deprotonation via **4b**-TS-Prt-1, rotated to bind the amine to the metal in **1b**-Ru-HemAm-2,[68] and then deprotonated via **4b**-TS-Prt-2 to give the amine-coordinated hemiaminaloxide ion-pair (**4b**-IP-NHMe). The latter ion-pair still needs to undergo aldehyde elimination to complete a metathesis. As discussed in Figure 3, C−NHMe bond cleavage

dx.doi.org/10.1021/ic500743u | Inorg. Chem. 2014, 53, 8334−8349

starting from **4b**-IP-NHMe proceeds by a distinct TS (**4b**-TS-NHMe) with $G^{\ddagger}_{rel}$ = 26.4 kcal/mol.

IRC calculations confirm the connectivities associated with a localized proton transfer originating from the C−H bound **3b**-TS-Prt-1 and **4b**-TS-Prt-1. Likewise, for the NHMe-bound deprotonation of the hemiaminal by **1**-Ru, the IRC starting from **4b**-TS-Prt-2 converges into the expected hemiaminal precomplex in one direction and the NHMe-bound ion-pair of the hemiaminaloxide in the other (blue line in Figure 9).

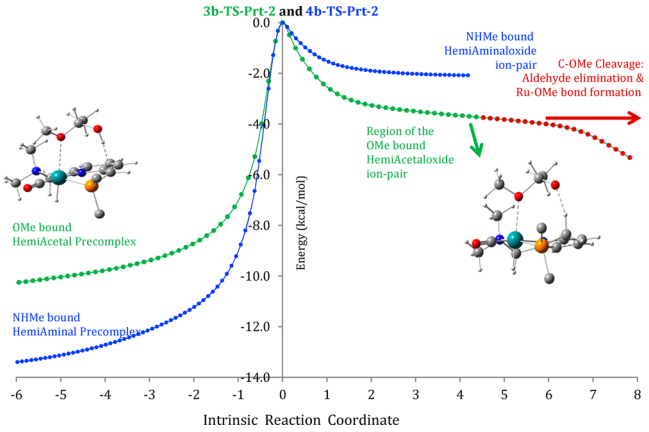

Figure 9. Intrinsic reaction coordinates originating from **3b**-TS-Prt-2 (hemiacetal; green curve) and **4b**-TS-Prt-2 (hemiaminal; blue curve). M06 gas phase electronic energies defined relative to the TSs in kcal/mol.

For the reaction of the OMe-bound hemiacetal on the other hand, the IRC originating from **3b**-**TS**-Prt-2 converges to the OMe bound hemiacetal precomplex in one direction, but it reaches a plateau in the direction of the OMe bound ion-pair and then proceeds with elimination of the aldehyde (Figure 9). This result enforces the proposition that once the OMe group of the hemiacetaloxide anion gets in the vicinity of the metal there will be no barrier to C−OMe cleavage and Ru-alkoxide formation. In spite of the lack of a distinct TS for C−OMe cleavage, the IRC from **3b**-TS-Prt-2 in Figure 9 is still most consistent with a dehydrogenation mechanism of the hemiacetaloxide in which the proton is transferred separately from C−OMe cleavage. We emphasize that the calculations do identify a true minimum for the OMe-bound hemiacetaloxide ion-pair on path **b** (**3b**-IP-OMe in Figure 8). This minimum is very shallow, and we argue it is best viewed as an activated species on the PES that undergoes a barrierless C−OR bond cleavage. To some extent therefore, the **3a**-TS-Slip-1 is effectively like a concerted metathesis TS.

Energy of the Slippage and MLC TSs. Table 2 compares the energies of the slippage and the C−H-bound proton transfer TSs in the reactions of **3** and **4** using different density functionals and solvent continuums. For the ester, the M06L $G^{\ddagger}_{rel}$ of **3b**-TS-Prt-1 in toluene (23.8 kcal/mol) is slightly higher than **3a**-TS-Slip-1 (21.8 kcal/mol). For *N*-methylacetamide on the other hand, the M06L $G^{\ddagger}_{rel}$ of **4b**-TS-Prt-1 is 28.3 kcal/mol,[69] 1.9 kcal/mol *lower* than $G^{\ddagger}_{rel}$ of **4a**-TS-Slip-1 (30.2 kcal/mol; in toluene continuum). The ωB97X-D or the M06L levels selectively stabilizes the proton transfer TSs (to 24.2 kcal/mol), thus increasing the preference for **4b**-TS-Prt-1 over **4a**-TS-Slip-1 to 4.6 kcal/mol (in toluene; Table 2). The results are not changed when full geometry minimization and normal-mode analysis are done at the ωB97X-D level.

Table 2. $G^{\ddagger}_{rel}$ of TS-Slip-1 and TS-Prt-1 at Different Theoretical Levels (in kcal/mol)

	ester reactions		carboxamide reactions	
	3a-TS-Slip-1	**3b**-TS-Prt-1	**4a**-TS-Slip-1	**4b**-TS-Prt-1
M06 (toluene)[a]	16.9	21.8	30.0	26.2
M06L (toluene)[a]	**21.8**	**23.8**	**30.2**	**28.3**
ωB97X-D (toluene)[a]	20.9	20.4	29.6	24.2
M06L (THF)[a]	23.6	26.3	31.8	31.5
M06L (methanol)[a]	14.8	24.2	28.2	30.9
Opt M06-L (Tol)[b]	21.6	23.3	30.0	27.6
Opt ωB97X-D (Tol)[c]	20.8	21.3	29.9	24.7
(*S1*) M06L (Tol)[a]	17.7	19.5	24.9	25.3

[a]Results from single-point calculations on geometries minimized in the gas phase at the M06 level. [b]Geometries and frequencies computed in the gas phase at the M06L level. [c]Geometries and frequencies computed in the gas phase at the ωB97X-D level.

The computed reversal in the energy order of the direct slippage and ligand deprotonation TSs in the reaction of the carboxamide compared to the reaction of the ester follows in part from a significantly larger proton affinity of the hemiaminaloxide anion compared to the hemiacetaloxide ($\Delta\Delta G^{\circ}$ = −6.4 kcal/mol; eq 21; favoring proton transfer in

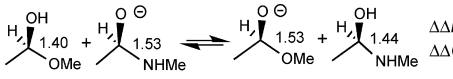

(21)

the reaction of **4**), and in part from a slightly larger barrier for rearrangement from IP-H to TS-Slip-1 in the carboxamide case ($\Delta\Delta G^{\ddagger}$ = 1.4 kcal/mol; Figure 1; disfavoring slippage in the reaction of **4**).

Given the ion-pair and acid−base nature of the given transformations, the precise contribution of the two paths to metathesis is expected to depend on dynamics and solvent effects details.[70] Such effects can be different for the two routes, but they are difficult to compute accurately. Thus, when a THF solvent continuum is used in the calculations, the M06L energies of **4a**-TS-Slip-1 and **4a**-TS-Prt-1 become nearly identical (Table 2), and in a methanol continuum the slippage TS becomes lower than the proton transfer TS by 2.7 kcal/mol. Furthermore, when a methanol molecule is included as an explicit H-bond donor in the calculations, the M06L **4a**-TS-Slip-1 becomes 0.4 kcal/mol *lower* than **4b**-TS-Prt-1 even in the toluene continuum (*S1* entries in Figures 7 and 8). We stress that the two TSs being compared are on two PESs leading to the same OR- or NHR-bound hemiacetaloxide and hemiaminaloxide ion-pairs, which we propose to activate the C−OR and C−NHR bonds in preparation for aldehyde elimination to complete an H/OR or H/NHR metathesis. In fact at the ωB97X-D level the barrier to C−NHMe cleavage on the MLC path via **4b**-TS-NHMe discussed in Figure 3 is 29.6 kcal/mol, significantly higher than that via **4b**-TS-Prt-1 (24.2 kcal/mol) and identical to that via **4a**-TS-Slip-1. The OR- and NHR-bound ion-pairs were not identified in previous computational studies of the MLC mechanisms. Consideration of these ion-pairs gives a fundamentally new perspective to understanding the metal-catalyzed C−OR and C−NHR bond cleavage step in the reaction of **2**-Ru-H with **3** and **4** regardless of how the IPs

dx.doi.org/10.1021/ic500743u | *Inorg. Chem.* 2014, 53, 8334−8349

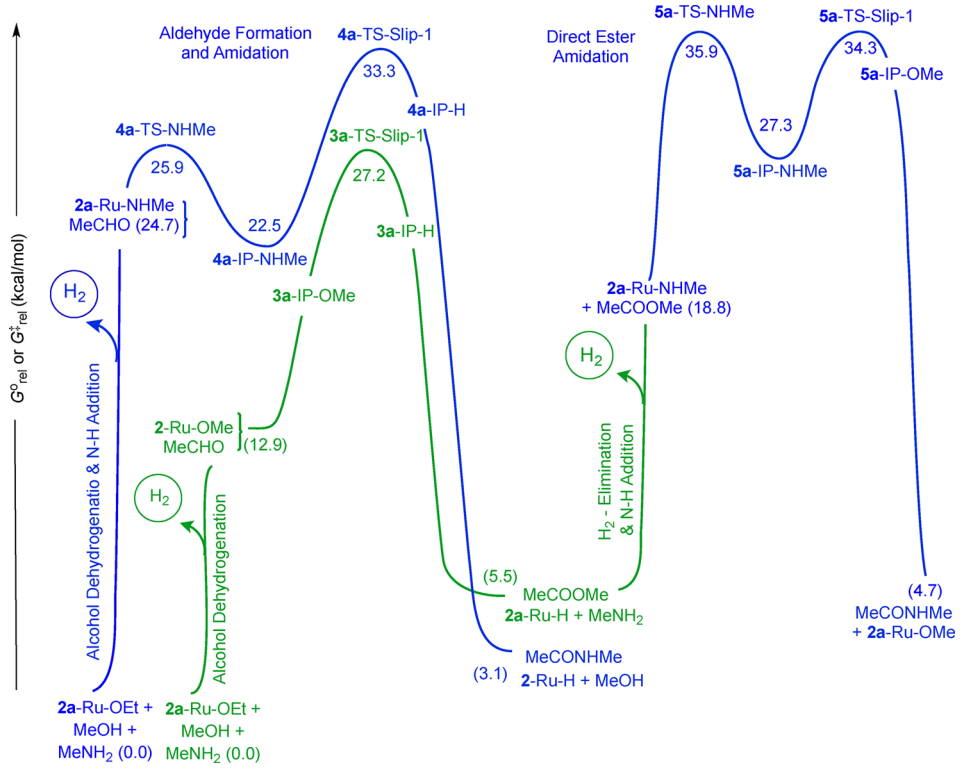

Figure 10. Standard state Gibbs free energy profiles (298 K; 1 atm) for dehydrogenative coupling starting with **1**-Ru in a mixture of methanol, ethanol and methylamine (M06L-toluene; in kcal/mol).

are formed. In addition to the slippage and MLC rearrangement modes, one can envision other routes to obtain the OR and NHR ion-pairs, such as by full dissociation and reassociation of the ion-pairs, formation of solvent separated ion-pairs, or by a protonation and deprotonation sequence of the anion by the alcohol that is produced during hydrogenation. Again, the contribution of such routes will depend on solvent and dynamics effects that may vary as the concentration of the alcohol is changed during the course of catalytic hydrogenation. The reaction via TS-Slip-1 provides sort of the least action path to rearrange the ion-pairs. The data in Table 2 shows this path to be at least competitive with the MLC mechanism involving ligand deprotonation and reprotonation.

Metathesis in the Dehydrogenative Coupling Direction. In this section we discuss the ion-pair PESs in the context of amine dehydrogenative coupling. To be able to address the question of the observed selectivity to carboxamides using the same data for methyl acetate and *N*-methylacetamide hydrogenation, we start with **1**-Ru in a mixture of ethanol, methanol, and methylamine. The computed free energy of ethanol addition to **1**-Ru is −6.9 kcal/mol, compared to −5.0 and +6.8 kcal/mol for methanol and methylamine addition, respectively. According to these results the resting state of the catalyst in the given mixture should be the octahedral ruthenium−ethanoxide (**2a**-Ru-OEt), so we place this complex along with methanol and methylamine at the zero level on the Gibbs free energy scale in Figure 10.

To produce methyl acetate from the given mixture, the mechanism under consideration requires a preparatory stage in which **2a**-Ru-OEt is dehydrogenated into acetaldehyde and H_2 along with the formation of **2**-Ru-OMe (similar to the preparatory stage in Scheme 1 in the Introduction). The thermodynamics of this stage is uphill by 12.9 kcal/mol. Again, for our purposes we can ignore the barriers in the preparatory stage. Coupling between the aldehyde and **2a**-Ru-OMe to give the C−OMe-bound hemiacetaloxide ion-pair is exothermic by 1.1 kcal/mol, but because of the unfavorable entropy term, the step is uphill by 6.0 kcal/mol (Figure 1), so G^{o}_{rel} of **3a**-IP-OMe in Figure 10 is 19.5 kcal/mol. To eliminate an ester, the hemiacetaloxide must rearrange to orient the C−H bond toward the metal. The rearrangement barrier from the shallow **3a**-IP-OMe via **3a**-TS-Slip-1 is 8.3 kcal/mol. **3a**-TS-Slip-1 is the highest energy point on the given PES, with a $G^{‡}_{rel}$ value of 27.2 kcal/mol. The thermodynamics for transformation from the initial reactants into **2**-Ru-H and the ester is uphill by 5.5 kcal/mol.

To form *N*-methylacetamide from the initial mixture in Figure 10, the preparatory stage requires dehydrogenation of **2a**-Ru-OEt as well as reaction of the amine to give **2a**-Ru-NHMe. Because the thermodynamics of amine addition to **1**-Ru is unfavorable (Table 1), the energy input for this stage is large: 24.7 kcal/mol. Coupling of aldehyde with **2a**-Ru-NHMe into **4a**-IP-NHMe encounters a small barrier estimated at 1.2 kcal/mol in Figure 1, but opposite to the reaction of **2a**-Ru-OMe, the coupling involving C−N bond formation is *exoergic* by 2.1 kcal/mol. However, the slippage barrier of the hemiaminaloxide needed to reach the C−H ion-pair is substantial (10.7 kcal/mol), so **4a**-TS-Slip-1 comes to 33.3 kcal/mol on the PES. The combined results indicate strongly therefore that, at least for the given substrates, dehydrogenative coupling into an ester should be kinetically much more favored than coupling into a carboxamide ($\Delta\Delta G^{‡}_{rel}$ = 6.1 kcal/mol). When the respective MLC routes are considered, the highest energy points on the two coupling PESs will be **3b**-TS-Prt-1 and **4b**-TS-Prt-1 with $G^{‡}_{rel}$ = 29.2 and 31.4 kcal/mol, respectively, still in favor of ester formation. Note that **4a**-IP-

dx.doi.org/10.1021/ic500743u | *Inorg. Chem.* 2014, 53, 8334−8349

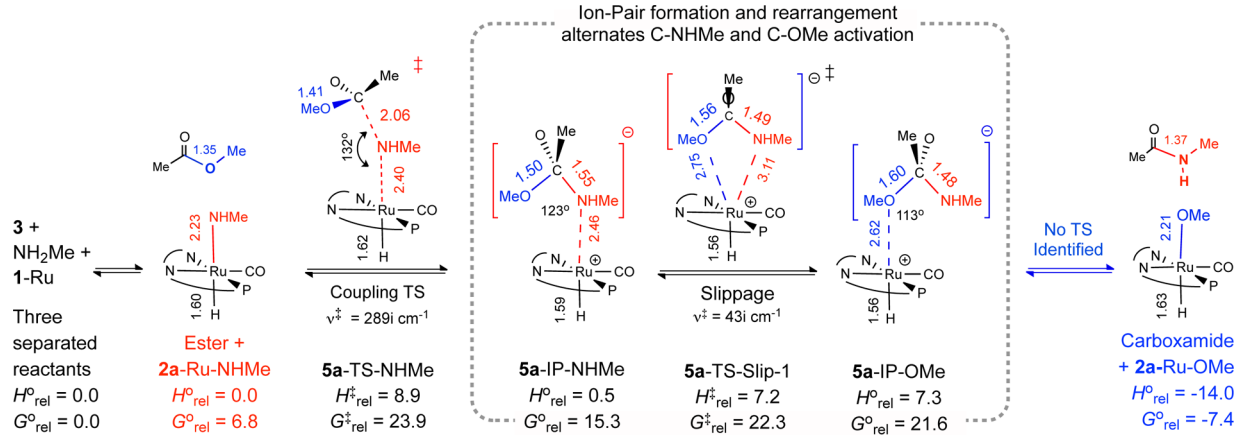

Figure 11. Stationary points on the outer-sphere PES in the reaction of an ester (**3**) and **2**-Ru-NHMe. Energies are given in kcal/mol relative to the separated reactants (M06L-toluene).

H in Figure 10 is 4.6 kcal/mol above **3a**-IP-H. These C−H ion-pairs are effectively the TSs for the final hydride transfer steps needed to eliminate the carboxamide or the ester. As such, it is unlikely there can be other metal-catalyzed mechanisms to coupling involving aldehydes that would selectively favor the population of the higher energy **4a**-IP-H to give a carboxamide as a kinetic product.

The computed kinetic preference to the ester in Figure 10 is opposite to the experimentally observed selectivity to carboxamides. However, the carboxamide is the thermodynamically favored product in the Figure ($\Delta\Delta G^{\circ}_{rel}$ = −2.4 kcal/mol). It is possible, therefore, that the ester can in practice be formed as a kinetic product, but it gets amidated under the experimental conditions, a possibility that had been raised in the studies by Milstein. As mentioned in the Introduction, complexes related to **1**-Ru are indeed known to catalyze ester amidation (eq 4), an interesting and valuable reaction in its own.[4]

Ester amidation under the alcohol-amine coupling conditions can in principle proceed on the same PESs involving the aldehyde. This will require the ester and **2**-Ru-H products to revert back to acetaldehyde and **2a**-Ru-OMe so the acetaldehyde may react with **2a**-Ru-NHMe to form the thermodynamically more favored carboxamide. In Figure 11 we give evidence for the accessibility of an alternative ion-pair NHR/OR metathesis route that achieves ester amidation in a more direct way.

Ester Amidation via NHR/OR Metathesis. The energies in Figure 11 are defined relative to the separated square pyramidal **1**-Ru, methylamine and methyl acetate, thus mimicking the initial conditions of an ester amidation experiment utilizing an alkyl amine. From this mixture the preparatory stage for an NHR/OR metathesis of the ester involves only methylamine addition to **1**-Ru, so the required energy input is relatively small, 6.8 kcal/mol. Coupling between the ester and **2**-Ru-NHMe gives an amine-coordinated ion-pair minimum of the *α*,*α*-(NHMe)(OMe)-ethanoxide anion (**5a**-IP-NHMe). The thermodynamics of the coupling step is computed to be nearly thermoneutral (ΔH°_{Add} = 0.5 kcal/mol), affording ΔG°_{Add} = 8.5 kcal/mol, but the step has a relatively high barrier via **5a**-TS-NHMe with $\Delta H^{\ddagger}_{Add}$ and $\Delta G^{\ddagger}_{Add}$ of 8.9 and 17.1 kcal/mol, respectively. **5a**-TS-NHMe is characterized by a C−N bond distance of 2.06 Å and $\nu^{\ddagger}$ = 289i cm^{-1} for C−N stretching vibration. Subsequent slippage via **5a**-TS-Slip-1 in Figure 11 rearranges the *α*,*α*-(NHMe)(OMe)-ethanoxide within the intact ion-pair to coordinate the methoxy group to the metal (**5a**-IP-OMe). The switch from NHMe to OMe coordination causes a contraction in the C−NHMe bond from 1.55 to 1.48 Å, and a stretch in the C−OMe bond from 1.50 to 1.60 Å, demonstrating again that metal-coordination activates the respective bonds. From **5a**-IP-OMe, cleavage of the C−OMe bond into **2a**-Ru-OMe and *N*-methylacetamide is highly exoergic (ΔG°_{Diss} = −29.7 kcal/mol), and a PES scan reveals the reaction to be totally barrierless. The net transformation in Figure 11 is an ion-pair-mediated metathesis in which an amide and alkoxide are exchanged between a ruthenium amide and an ester. Unlike the metatheses involving H/OR, H/NHR (Figure 1) or OR/OR exchange,[33] the highest energy point on the NHMe/OMe metathesis PES in Figure 11 is for the TS of the ester−amide coupling step, and not the slippage TS. The difference between the two TSs is however small (23.9 vs 22.3 kcal/mol). Thus, ester amidation is highly exoergic, and the direct metal-mediated metathesis route provides a surprisingly low energy barrier for the transformation.

In studying ester amidation, we also considered the MLC route to an NHR/OR ion-pair rearrangement. The transition state for ligand deprotonation on path **b** via the NHMe-coordinated *α*,*α*-(NHMe)(OMe)-ethanoxide (**5b**-TS-Prt-1; eq 22) has G°_{rel} = 22.6 kcal/mol, similar to **5a-TS**-Slip-1 (22.3 kcal/mol; M06L-toluene). However, the TS for ligand reprotonation via the OMe-coordinated anion (**5b**-TS-Prt-2; eq 22) is 26.3 kcal/mol, indicating the MLC route is overall less favored than ion-pair slippage.

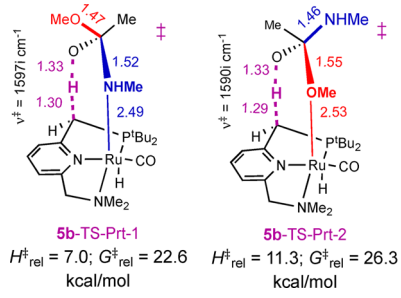

(22)

When considered in the context of amine-alcohol coupling discussed in Figure 10, ester amidation has to start from **2**-Ru-H, the ester, and the free amine. The energy of the latter

dx.doi.org/10.1021/ic500743u | Inorg. Chem. 2014, 53, 8334−8349

species on the scale in Figure 10 is 5.5 kcal/mol. The preparatory stage for ester amidation requires H_2 elimination and **2**-Ru-NHMe formation, with an energy input of 13.4 kcal/mol. This puts **5a**-TS-NHMe and **5a**-TS-Slip-1 at 35.9 and 34.4 kcal/mol, slightly higher than **4a-TS**-Slip-1 (33.3 kcal/mol) for ester amidation via the (reversible) aldehyde route. However, the energy scale in Figure 10 applies to a condition where each species, including H_2, is present under standard state conditions (1 atm and 298 K). Experimentally, coupling is possible only because H_2 is liberated from the reaction mixture under reflux, so taking the energy of the "final" ester product as +5.5 kcal/mol on the amidation NHR/OR PES in Figure 10 is clearly not representative of the catalytic system, and the contribution of the direct NHR/OR route may in practice be much greater than the one suggested by the standard state energy profile. To put it differently, because H_2 is removed from the reaction mixture under dehydrogenative coupling conditions, rehydrogenolysis of the ester into an aldehyde and an alcohol becomes less likely, leaving the ester/amine coupling route as the "only" remaining option for carboxamide formation. Interestingly, if esters are produced and amidated in the dehydrogenative coupling of amines into carboxamides, esters can in turn be produced and hydrogenated in the reverse *hydrogenation* of carboxamides starting with **2**-Ru-H. This most unusual inference should of course be valid independent of the true mechanism of ester amidation. In the ion-pair slippage framework, carboxamide hydrogenation would initially proceed by the H/NHR metathesis route described in Figure 1. As the reaction proceeds, the concentration of the alcohol will increase. If the equilibrium concentration of **2a**-Ru-OR under H_2 becomes significant, it can undergo an OR/NHR metathesis with the carboxamide to give an ester and **2a**-Ru-NHR. **2a**-Ru-NHR will give the amine hydrogenation product. Figure 1 establishes that hydrogenation of the ester using **2**-Ru-H should be comparatively fast, so this will give the second hydrogenation (alcohol) product of the initial carboxamide.

CONCLUSIONS

Based on detailed electronic structure calculations, the present study proposes that the dehydrogenative coupling of amines with alcohols or esters into carboxamides that can be catalyzed by Milstein's d^6-[Ru(PNN)(CO)(H)] catalysts (**1**-Ru) can be understood in terms of simple metal/acyl metathesis transformations. The study assumes that alcohol dehydrogenation into aldehydes is an accessible transformation in the given systems. We start with the observation that complexes related to **1**-Ru undergo characteristic metal−ligand cooperative (heterolytic) addition of H_2, ROH and NH_2R to give octahedral d^6-ruthenium complexes (**2**-Ru-X) in which a hydride, alkoxide, or an amide is positioned trans to a hydride (Scheme 6).

Hydride transfer from a metal complex such as **2**-Ru-H to a carbonyl group is familiar. Our idea is that the coordinated alkoxide and amide anions (X^-) of the other octahedral complexes can undergo similar reactions with an aldehyde or an ester (RCYO). The immediate product from such reactions on the PES is an uphill contact ion-pair of an α-substituted alkoxide anion ($RCXYO^-$) in which the newly formed C−X bond is coordinated to the metal (X-ion-pair). The coordination of the X group appears to activate the corresponding C−X bond. At first there appears to be nothing unusual or remarkable about the given "transfer" or "coupling" steps. However, if we accept that X can move from **2**-Ru-X to

Scheme 6. X/Y - metal/acyl metathesis

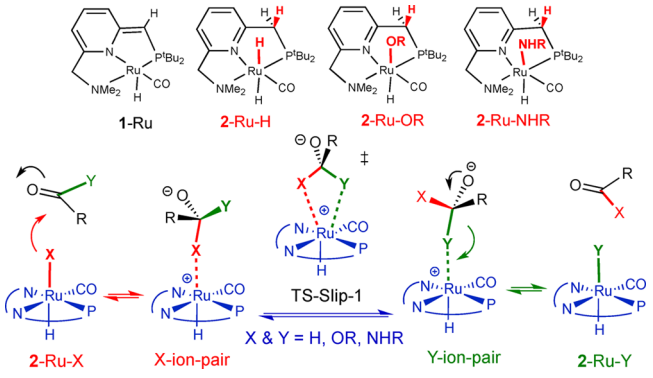

an organic acyl-Y molecule, it becomes evident that the same reaction can take place in reverse from the α-substituted alkoxide via Y. This produces a new octahedral ruthenium complex (**2**-Ru-Y) and a new organic acyl-X product. The net reaction is a novel metathesis in which X and Y are interchanged between a metal and an acyl group. This simple reaction can be readily used to rationalize much of Milstein's extraordinary chemistry. All is needed here is a trivial rotation of the α,α-(X)(Y)-substituted alkoxide to orient Y in the direction of the metal. The calculations show the process can take place in a least action mode via TS-Slip-1. The characterization of the individual X or Y transfer regions on the PES proved to be a tedious exercise in locating shallow ion-pair minima and elusive flat TSs that can easily be absent from the PES. At the end, the results reveal the H/OR and H/HNR slippage TSs to be the highest energy point on the metathesis PES. For these cases the full metathesis PES is in effect like a single concerted step taking place via TS-Slip-1. For the NHR/OR metathesis on the other hand, the highest energy point is the TS for C−N coupling between the ester and metal-coordinated amide, but this is only slightly higher than the slippage TS. If it occurs without a barrier, ion-pair dissociation into free ions and reassociation by a different group would provide a variation to the ion-pair rearrangement mechanism that would circumvent the slippage TS.

The present study shows that the hydrogenation MLC mechanism involving hemiacetal and hemiaminal formation followed by a metal mediated fragmentation is simply an indirect multistep route to the same metathesis that can be mediated by ion-pair rearrangement. The MLC and ion-pair slippage routes to metathesis are computed to be competitive. A definitive theoretical comparison of the possible role of the different routes to the same reaction in catalysis requires dynamics effects and accurate estimates of both the basicity of the α-substituted alkoxides and solvation of the ion-pair, which are not easy to evaluate computationally. We demonstrate for example that changing the solvent continuum from toluene to THF or methanol, or including a methanol molecule explicitly in the calculations shift the results in favor of the ion-pair slippage route. These computed results cannot rule out a role for MLC in catalysis, but at the same time they do indicate that the more direct slippage route is also plausible. Taken at face value, our results based on conventional transition state theory and implicit bulk treatment of solvation indicate that the dehydrogenative coupling of methyl amines with ethanol using **1**-Ru proceeds by initial formation of an ester via an ion-pair OR/H metathesis followed by ester amidation via a low energy ion-pair NHR/OR metathesis.

dx.doi.org/10.1021/ic500743u | Inorg. Chem. 2014, 53, 8334−8349

■ ASSOCIATED CONTENT

Supporting Information

Tables of absolute energies and Cartesian coordinates, and a separate.txt file. Changing the extension of this file from.txt to.mol2 allows direct visualization of all of the molecules using the Mercury free software. This material is available free of charge via the Internet at http://pubs.acs.org.

■ AUTHOR INFORMATION

Corresponding Author

*E-mail: fh19@aub.edu.lb

Notes

The authors declare no competing financial interest.

■ ACKNOWLEDGMENTS

This work was supported by the University Research Board of the American University of Beirut. The calculations were done on the HPC computer at AUB. Additional resources were provided by the IT Research Computing group in *Texas A&M University at Qatar*, supported by the *Qatar Foundation for Education, Science and Community Development.*

■ DEDICATION

This study is dedicated to Professor Andrew Streitwieser for his pioneering contributions in ion-pair chemistry.

■ REFERENCES

(1) (a) Zhang, J.; Leitus, G.; Ben-David, Y.; Milstein, D. *J. Am. Chem. Soc.* **2005**, *127*, 10840. (b) Zhang, J.; Balaraman, E.; Leitus, G.; Ben-David, Y.; Milstein, D. *Organometallics* **2011**, *30*, 5716.

(2) (a) Gunanathan, C.; Ben-David, Y.; Milstein, D. *Science* **2007**, *317*, 790. (b) Gunanathan, C.; Milstein, D. *Angew. Chem., Int. Ed.* **2008**, *47*, 8661. (c) Khusnutdinova, J. R.; Ben-David, Y.; Milstein, D. *Adv. Synth. Catal.* **2013**, *355*, 3525.

(3) (a) Zeng, H.; Guan, Z. *J. Am. Chem. Soc.* **2011**, *133*, 1159. (b) Gnanaprakasam, B.; Balaraman, E.; Gunanathan, C.; Milstein, D. *J. Polym. Sci., Part A: Polym. Chem.* **2012**, *50*, 1755.

(4) (a) Gnanaprakasam, B.; Ben-David, Y.; Milstein, D. *Adv. Synth. Catal.* **2010**, *352*, 3169. (b) Srimani, D.; Balaraman, E.; Gnanaprakasam, B.; Ben-David, Y.; Milstein, D.; Leitner, W. *Adv. Synth. Catal.* **2012**, *354*, 2403.

(5) (a) Gnanaprakasam, B.; Milstein, D. *J. Am. Chem. Soc.* **2011**, *133*, 1682. (b) Barrios-Francisco, R.; Balaraman, E.; Diskin-Posner, Y.; Leitus, G.; Shimon, L. J. W.; Milstein, D. *Organometallics* **2013**, *32*, 2973.

(6) (a) Milstein, D. *Top. Catalysis* **2010**, *53*, 915. (b) Gunanathan, C.; Milstein, D. *Top. Organomet. Chem.* **2011**, *37*, 55.

(7) (a) Ito, M.; Ootsuka, T.; Watari, R.; Shibashi, A.; Himizu, A.; Ikariya, T. *J. Am. Chem. Soc.* **2011**, *133*, 4240. (b) Dub, P. A.; Ikariya, T. *ACS Catal.* **2012**, *2*, 1718. (c) Clarke, M. L. *Catal. Sci. Technol.* **2012**, *2*, 2418.

(8) (a) Zeng, H.; Guan, Z. *J. Am. Chem. Soc.* **2011**, *133*, 1159. (b) Gnanaprakasam, B.; Balaraman, E.; Gunanathan, C.; Milstein, D. *J. Polym. Sci., Part A: Polym. Chem.* **2012**, *50*, 1755.

(9) (a) Zhang, J.; Leitus, G.; Ben-David, Y.; Milstein, D. *Angew. Chem., Int. Ed.* **2006**, *45*, 1113. (b) Zell, T.; Ben-David, Y.; Milstein, D. *Angew. Chem., Int. Ed.* **2014**, *53*, 4685.

(10) Balaraman, E.; Gnanaprakasam, B.; Shimon, L. J. W.; Milstein, D. *J. Am. Chem. Soc.* **2010**, *132*, 16756.

(11) (a) de Vries, J. G.; Elsevier, C. J. *The Handbook of Homogeneous Hydrogenation*; Wiley-VCH: Weinheim, Germany, 2007. (b) Noyori, R.; Hashiguchi, S. In *Applied Homogeneous Catalysis with Organometallic Compounds*; Wiley-VCH Verlag GmbH: New York, 2008. (c) Noyori, R. *Asymmetric Catalysis in Organic Synthesis*; Wiley: New York, 1994.

(12) Trost, B. M., Fleming, I., Eds. *Comprehensive Organic Synthesis*; Pergamon, New York, 1991; Vol. *8*.

(13) (a) Seyden-Penne, J. *Reductions by the Alumino- and Borohydrides in Organic Synthesis*, 2nd ed.; Wiley: New York, 1997. (b) Gribble, G. W. *Chem. Soc. Rev.* **1998**, *27*, 395.

(14) Balaraman, E.; Gunanathan, C.; Zhang, J.; Shimon, L. J. W.; Milstein, D. *Nat. Chem.* **2011**, *3*, 609.

(15) Balaraman, E.; Ben-David, Y.; Milstein, D. *Angew. Chem., Int. Ed.* **2011**, *50*, 11702.

(16) (a) Ito, M.; Ootsuka, T.; Watari, R.; Shiibashi, A.; Himizu, A.; Ikariya, T. *J. Am. Chem. Soc.* **2011**, *133*, 4240. (b) Dub, P. A.; Ikariya, T. *ACS Catal.* **2012**, *2*, 1718.

(17) Gunanathan, C.; Milstein, D. *Acc. Chem. Res.* **2011**, *44*, 588.

(18) Gunanathan, C.; Milstein, D. *Science* **2013**, *341*, 249.

(19) (a) Noyori, R.; Hashiguchi, S. *Acc. Chem. Res.* **1997**, *30*, 97. (b) Noyori, R. *Angew. Chem., Int. Ed.* **2002**, *41*, 2008.

(20) (a) Clapham, S. E.; Hadzovic, A.; Morris, R. H. *Coord. Chem. Rev.* **2004**, *248*, 2201. (b) Joseph, S. M.; Samec, J. S.; Backvall, J.-E.; Andersson, P. G. *Chem. Soc. Rev.* **2006**, *35*, 237. (c) Dobereiner, G. E.; Crabtree, R. H. *Chem. Rev.* **2010**, *110*, 681. (d) Eisenstein, O.; Crabtree, R. H. *New. J. Chem.* **2013**, *37*, 21.

(21) Wiberg, K. B.; Morgan, K. M.; Maltz, H. *J. Am. Chem. Soc.* **1994**, *116*, 11067.

(22) Carey, F. A. *Organic Chemistry*, 6th ed.; McGraw Hill Inc.: New York, 2006; Chapter 17.

(23) (a) Roundhill, D. M. *Chem. Rev.* **1992**, *92*, 1. (b) Hamid, M. H. S. A.; Slatford, P. A.; Williams, J. M. J. *Adv. Synth. Catal.* **2007**, *349*, 1555. (c) Fujita, K.; Fujii, T.; Yamaguchi, R. *Org. Lett.* **2004**, *6*, 3525. (d) Yamaguchi, R.; Kawagoe, S.; Asai, C.; Fujita, K. *Org. Lett.* **2008**, *10*, 181. (e) Tillack, A.; Hollmann, D.; Michalik, D.; Beller, M. *Tetrahedron Lett.* **2006**, *47*, 8881. (f) Hollmann, D.; Tillack, A.; Michalik, D.; Jackstell, R.; Beller, M. *Chem.—Asian J.* **2007**, *2*, 403. (g) Hamid, M. H. S. A.; Williams, J. M. J. *Chem. Commun.* **2007**, 725.

(24) (a) Balcells, D.; Nova, A.; Clot, E.; Gnanamgari, D.; Crabtree, R. H.; Eisenstein, O. *Organometallics* **2008**, *27*, 2529. (b) Nova, A.; Balcells, D.; Dobereiner, G. H.; Crabtree, R. H.; Eisenstein, O. *Organometallics* **2010**, *29*, 6548.

(25) Gnanaprakasam; Zhang, J.; Milstein, D. *Angew. Chem., Int. Ed.* **2010**, *49*, 1468.

(26) (a) Li, H.; Wang, X.; Huang, F.; Lu, G.; Jiang, J.; Wang, Z.-X. *Organometallics* **2011**, *30*, 5233. (b) Li, H.; Wen, M.; Wang, Z. X. *Inorg. Chem.* **2012**, *51*, 5716. (c) Li, H.; Wang, X.; Wen, M.; Wang, Z.-X. *Eur. J. Inorg. Chem.* **2012**, *2012*, 5011. (d) Cho, D.; Ko, K. C.; Lee, J. Y. *Organometallics* **2013**, *32*, 4571. (e) Qu, S.; Dang, Y.; Song, C.; Wen, M.; Huang, K.-W.; Wang, Z. *J. Am. Chem. Soc.* **2014**, *136*, 4947.

(27) (a) Zeng, G.; Li, S. *Inorg. Chem.* **2011**, *50*, 10572. (b) Cantillo, D. *Eur. J. Inorg. Chem.* **2011**, *19*, 3008.

(28) (a) Iron, M. A.; Ben-Ari, E.; Cohen, R.; Milstein, D. *Dalton Trans.* **2009**, 9433. (b) Schwartsburd, L.; Iron, M. A.; Konstantinovski, L.; Diskin-Posner, Y.; Leitus, G.; Shimon, L. J. W.; Milstein, D. *Organometallics* **2010**, *29*, 3817.

(29) (a) Tomasi, J.; Mennucci, B.; Cances, E. *J. Mol. Struct. (THEOCHEM)* **1999**, *464*, 211. (b) Yang, X. *ACS Catal.* **2012**, *2*, 964. (c) Yang, X. *ACS Catal.* **2013**, 2684. (e) Sandhya, K. S.; Suresh, C. H. *Organometallics* **2013**, *32*, 2926. (d) Li, H.; Hall, M. B. *J. Am. Chem. Soc.* **2014**, *136*, 383.

(30) (a) Basolo, F.; Pearson, R. G. *Prog. Inorg. Chem.* **1962**, *4*, 381. (b) Appleton, T. G.; Clark, H. C.; Manzer, L. E. *Coord. Chem. Rev.* **1973**, *10*, 335. (c) Coe, B. J.; Glenwright, S. J. *Coord. Chem. Rev.* **2000**, *203*, 5. (d) Appleton, T. G.; Bennett, M. A. *Inorg. Chem.* **1978**, *17*, 738. (e) Appleton, T. G.; Hall, J. R.; Ralph, S. F. *Inorg. Chem.* **1985**, *24*, 4685. (f) Weinhold, F.; Landis, C. R. *Valency and Bonding: A Natural Bond Orbital Donor-Acceptor Perspective*; Cambridge University Press: Cambridge, 2005.

(31) (a) Hasanayn, F.; Abu-El-Ez, D. *Inorg. Chem.* **2010**, *49*, 9162. (b) Hasanayn, F.; Achord, P.; Braunstein, P.; Magnier, H. J.; Krogh-Jespersen, K.; Goldman, A. S. *Organometallics* **2012**, *31*, 4680.

(32) Hasanayn, F.; Morris, R. H. *Inorg. Chem.* **2012**, *51*, 10808.

(33) Hasanayn, F.; Baroudi, A. *Organometallics* **2013**, *32*, 2493.

(34) Hasanayn, F.; Baroudi, A.; Bengali, A.; Goldman, A. S. *Organometallics* **2013**, *32*, 6969.
(35) Spasyuk, D.; Smith, S.; Gusev, D. G. *Angew. Chem., Int. Ed.* **2013**, *52*, 2538.
(36) Khaskin, E.; Iron, M. A.; Shimon, L. J. W.; Zhang, J.; Milstein, D. *J. Am. Chem. Soc.* **2010**, *132*, 8542.
(37) Frisch, M. J. et al.. *Gaussian 09*, Rev. A.02; Gaussian, Inc.: Wallingford, CT, 2009.
(38) Zhao, Y.; Truhlar, D. G. *Theor. Chem. Acc.* **2008**, *120*, 215.
(39) (a) McLean, A. D.; Chandler, G. S. *J. Chem. Phys.* **1980**, *72*, 5639. (b) Raghavachari, K.; Binkley, J. S.; Seeger, R.; Pople, J. A. *J. Chem. Phys.* **1980**, *72*, 650. (c) Rassolov, V. A.; Ratner, M. A.; Pople, J. A.; Redfern, P. C.; Curtiss, L. A. *J. Comput. Chem.* **2001**, *22*, 976.
(40) Hay, P. J.; Wadt, W. R. *J. Chem. Phys.* **1985**, *82*, 279.
(41) Höllwarth, A.; Böhlers, A. W.; Bohme, M.; Dapprich, S.; Gobbi, A.; Hollwarth, A.; Jonas, V.; Köhler, K. F.; Stegmann, R.; Veldkamp, A.; Frenking, G. *Chem. Phys. Lett.* **1993**, *208*, 111.
(42) See: https://bse.pnl.gov/bse/portal.
(43) Fukui, K. *Acc. Chem. Res.* **1981**, *14*, 363.
(44) Zhao, Y.; Truhlar, D. G. J. *Chem. Phys.* **2006**, *125*, 194101.
(45) Chai, J.-D.; Head-Gordon, M. *Phys. Chem. Chem. Phys.* **2008**, *10*, 6615.
(46) Marenich, A. V.; Cramer, C. J.; Truhlar, D. G. *J. Phys. Chem. B* **2009**, *113*, 6378.
(47) Averkiev, B. B.; Truhlar, D. G. *Catal. Sci. Technol.* **2011**, *1*, 1526.
(48) Gusev, D. G. *Organometallics* **2013**, *32*, 4239.
(49) Pudasaini, B.; Janesko, B. J. *Organometallics* **2014**, *33*, 84.
(50) Remya, K.; Suresh, C. H. *J. Comput. Chem.* **2013**, *34*, 1341.
(51) In conducting the present study we paid careful attention to the stereoisomeric, and diastereomeric details that can be generated when an ester or carboxamide is reacted with **2**-Ru-H in an outer-sphere mode. While we cannot claim we calculated every possibility, we think we have done enough to ensure that the reported results are representative of low energy profiles, sometimes by calculating three or four different stereoisomers for the same TS (which typically vary within 3 kcal/mol).
(52) Yang, X. *Inorg. Chem.* **2011**, *50*, 12836.
(53) Sandoval, C. A.; Ohkuma, T.; Muñiz, K.; Noyori, R. *J. Am. Chem. Soc.* **2003**, *125*, 13490.
(54) Casey, C. P.; Johnson, J. B.; Singer, S. W.; Cui, Q. *J. Am. Chem. Soc.* **2005**, *127*, 3100.
(55) (a) Hedberg, C.; Kallstrom, K.; Arvidsson, P. I.; Brandt, P.; Andersson, P. G. *J. Am. Chem. Soc.* **2005**, *127*, 15083. (b) Xin Zhang, X.; Guo, X.; Chen, Y.; Tang, Y.; Lei, M.; Fang, W. *Phys. Chem. Chem. Phys.* **2012**, *14*, 6003.
(56) Findlater, M.; Bernskoetter, W. H.; Brookhart, M. *J. Am. Chem. Soc.* **2010**, *132*, 4534.
(57) Takebayashi, S.; Bergens, S. H. *Organometallics* **2009**, *28*, 2349.
(58) (a) Baratta, W.; Chelucci, G.; Gladiali, S.; Siega, K.; Toniutti, M.; Zanette, M.; Zangrando, E.; Rigo, P. *Angew. Chem., Int. Ed.* **2005**, *44*, 6214. (b) Baratta, W.; Bosco, M.; Chelucci, G.; Del Zotto, A.; Siega, K.; Toniutti, M.; Zangrando, E.; Rigo, P. *Organometallics* **2006**, *25*, 4611. (c) Baratta, W.; Ballico, M.; Esposito, G.; Rigo, P. *Chem.—Eur. J.* **2008**, *14*, 558.
(59) (a) Hamilton, R. J.; Leong, C. G.; Bigam, G.; Miskolzie, M.; Bergens, S. H. *J. Am. Chem. Soc.* **2005**, *127*, 4152. (b) Hamilton, R. J.; Bergens, S. H. *J. Am. Chem. Soc.* **2006**, *128*, 13700. (c) Hamilton, R. J.; Bergens, S. H. *J. Am. Chem. Soc.* **2008**, *130*, 11979. (d) Takebayashi, S.; Dabral, N.; Miskolzie, M.; Bergens, S. H. *J. Am. Chem. Soc.* **2011**, *133*, 9666.
(60) (a) Bertoli, M.; Choualeb, A.; Lough, A. J.; Moore, B.; Spasyuk, D.; Gusev, D. G. *Organometallics* **2011**, *30*, 3479. (b) Spasyuk, D.; Gusev, D. G. *Organometallics* **2012**, *31*, 5239.
(61) (a) Darensbourg, D. J.; Rokicki, A.; Darensbourg, M. Y. *J. Am. Chem. Soc.* **1981**, *103*, 3223. (b) Darensbourg, D. J.; Kudaroski, R.; Bauch, C. G.; Pala, M.; Simmons, D.; White, J. N. *J. Am. Chem. Soc.* **1985**, *107*, 7463. (c) Darensbourg, D. J.; Kyran, S. J.; Yeung, A. D.; Bengali, A. A. *Eur. J. Inorg. Chem.* **2013**, 4024. (d) Whittlesey, M. K.; Perutz, R. N.; Moore, M. H. *Organometallics* **1996**, *15*, 5166.
(62) (a) Salem, H.; Shimon, L. J. W.; Diskin-Posner, Y.; Leitus, G.; Ben-David, Y.; Milstein, D. *Organometallics* **2009**, *28*, 4791. (b) Langer, R.; Diskin-Posner, Y.; Leitus, G.; Shimon, L. J. W.; Ben-David, Y.; Milstein, D. *Angew. Chem., Int. Ed.* **2011**, *50*, 9948.
(63) Schmeier, T. J.; Dobereiner, G. E.; Crabtree, R. H.; Hazari, N. *J. Am. Chem. Soc.* **2011**, *133*, 9274.
(64) Blum, O.; Milstein, D. *J. Organomet. Chem.* **2000**, *593*−*594*, 479.
(65) Smythe, N. A.; Grice, K. A.; Williams, B. S.; Goldberg, K. I. *Organometallics* **2009**, *28*, 277.
(66) Fafard, C. M.; Ozerov, O. V. *Inorg. Chim. Acta* **2007**, *360*, 286.
(67) Note that in the specific orientations considered in Figure 6 the exchanging C−H and C−O^- bonds are aligned roughly along the N−Ru−CO axis. The TSs in which the C−H and C−O^- groups are aligned along the amine−Ru−phosphine axis are calculated to be higher in energy by about 5 kcal/mol.
(68) The pairs of hemiacetal and hemiaminal precomplexes in Figure 8 are diasteromeric rotamers. We assume these are formed by dissociation of the precomplexes and reassociation in a different configuration. These specific pairs provide the lowest energy proton transfer TSs on the MLC path. The other pairs of diatereomers provide proton transfer TSs that are approximately 2 kcal/mol higher in energy.
(69) **4b**-TS-Prt-1 in Figure 8 has the lowest energy in a set of seven conformational or stereoisomeric TSs we computed in studying C−H deprotonation.
(70) Handgraaf, J.-W.; Meijer, E. J. *J. Am. Chem. Soc.* **2007**, *129*, 3099.